

An Investigation of Lean Premixed Hydrogen Combustion in a Gas Turbine Engine

Matthew Perry

Thesis submitted to the faculty of the
Virginia Polytechnic Institute and State University
in partial fulfillment of the requirements for the degree of

Master of Science
In
Mechanical Engineering

Walter F. O'Brien, Chair
Uri Vandsburger
Stephen D. LePera

June 22, 2009
Blacksburg, Virginia

Keywords: Hydrogen, Lean Premixed Combustion, Gas Turbine Engine,
Flashback, Stability Limit

An Investigation of Lean Premixed Hydrogen Combustion in a Gas Turbine Engine

Matthew Perry

(ABSTRACT)

As a result of growing concerns about the carbon emissions associated with the combustion of conventional hydrocarbon fuels, hydrogen is gaining more attention as a clean alternative. The combustion of hydrogen in air produces no carbon emissions. However, hydrogen-air combustion does have the potential to produce oxides of nitrogen (NO_x), which are harmful pollutants. The production of NO_x can be significantly curbed using lean premixed combustion, wherein hydrogen and air are mixed at an equivalence ratio (the ratio of stoichiometric to actual air in the combustion process) significantly less than 1.0 prior to combustion. Hydrogen is a good candidate for use in lean premixed systems due to its very wide flammability range. The potential for the stable combustion of hydrogen at a wide range of equivalence ratios makes it particularly well-suited to application in gas turbines, where the equivalence ratio is likely to vary significantly over the operating range of the machine.

The strong lean combustion stability of hydrogen-air flames is due primarily to high reaction rates and the associated high turbulent burning velocities. While this is advantageous at low equivalence ratios, it presents a significant danger of flashback—the upstream propagation of the flame into the premixing device—at higher equivalence ratios. An investigation has been conducted into the operation of a specific hydrogen-air premixer design in a gas turbine engine. Laboratory tests were first conducted to determine the upper stability limits of a single premixer. Tests were then carried out in which eighteen premixers and a custom-fabricated combustor liner were installed in a modified Pratt and Whitney Canada PT6A-20 turboprop engine. The tests examined the premixer and engine operability as a result of the modifications. A computer cycle analysis model was created to help analyze and predict the behavior of the modified engine and premixers. The model, which uses scaled component maps to predict off-

design engine performance, was integral in the analysis of premixer flashback which limited the operation of the modified engine.

ACKNOWLEDGEMENTS

First, I would like to thank Bruce Cambata and Joe Garst of Electric Jet, LLC, the sponsors of this research. I began my career as a graduate student with little more than a mild interest in turbomachinery, but, thanks to the opportunity to participate in the hydrogen turbine project, will finish it with a genuine desire to see the success of hydrogen as a part of our future. Bruce and Joe have been better sponsors than one could ask for, giving the research team their support but allowing us the freedom to act on our best judgment. What at first seemed like a terrifying amount of responsibility has turned out to be empowering and has helped to make me a better engineer.

I'd like to acknowledge Dr. Walter O'Brien, my advisor. Dr. O'Brien showed faith in my abilities by allowing me to choose this research and I can only hope that my accomplishments have justified that faith. He has always had time for me and my colleagues and has provided support and guidance, for which I am very grateful. I would also like to thank Dr. Uri Vandsburger for his support of the project, through both his insight and the use of the combustion lab. For his support at the airport lab, I'd like to thank Bill Hook, from whom I have learned a great deal about the practical aspects of gas turbines.

I would be remiss (although I'm not sure what that means—I should probably ask Jordan) if I failed to mention “Rescue Steve” LePera, whose contributions as a technician and engineer have been immeasurable. If anyone can be identified as an “idea man,” it's Steve, and when I come to the conclusion that giving up is the most efficient solution, he's always good for an idea that changes my mind. There's no one I'd rather have around when there's a chance of a Franceformer-related incident, but I have to hope that “Rusty Spoons” keeps its distance. Steve has been great to have around and is someone I'm happy to consider a friend.

That brings me to Jordan Farina, the unchallenged king of keeping things from shooting out of things. As a colleague, Jordan proves himself on a daily basis as a very intelligent, capable person who genuinely cares about our success. As a friend, Jordan is a great guy who always looks out for me (even when things get out of hand). Dan Villarreal has also been great to work with on a day-to-day basis. I'd like to think I work with Jordan more often than Dan because a controller is a one-man job, but a more likely explanation is that Dan's block diagrams make me want to cry. Regardless, Dan is always reliable and has been a great friend.

According with references, no one was a better friend to me in grad school than Capers "S" Thompson. On top of being a great room mate, Cape understands my particular brand of craziness the way only a handful of people do. We've had a lot of fun together, even if things drifted a little left of center 0.21 percent of the time. It's impossible to count the number of ways Cape helped make my day-to-day life easier, and I'm grateful for that. Bosco also deserves recognition, as his hilariously pathetic personality always put me in a good mood. I've rarely met an animal whose very existence made me laugh. Though his irrational fear of inanimate objects suggests that he may have been the one-time recipient of the ol' Crayola-Oblongata, no one was ever happier to see me when I walked in the door.

Last but not least, I'd like to thank my family. My brother, Jon, while disturbingly similar to me, has taught me a lot. I was glad to have him around during my first three years of college and wish him continued success on the West Coast. I appreciate my parents' continued support and the fact that they have always allowed me to pursue my interests. While my family as a whole may be mildly insane, I think I fit right in.

Table of Contents

Abstract	ii
Acknowledgements	iv
Table of Contents	vi
List of Figures	viii
List of Tables	xi
Chapter 1: Introduction	1
Chapter 2: Review of Literature	4
Chapter 3: Premixer and Combustor Liner Design	8
3.1 Premixer Design	8
3.2 Combustor Liner Design	11
Chapter 4: Research Plan	14
4.1 Combustion Lab Test Setup	14
4.2 Combustion Lab Test Strategy	17
4.3 Gas Turbine Lab Test Setup	21
4.4 Engine Test Strategy	24
4.5 Computational Engine Model	25
Chapter 5: Experimental and Computational Results	28
5.1 Results of the Premixer Tests	28
5.2 Discussion of Premixer Test Results	34
5.3 Results of the Engine Tests	35
5.4 Discussion of the Engine Test Results	40
5.5 Computer Model Results: Unmodified Engine Performance	41
5.6 Computer Model Results: Modified Engine Performance	46
5.7 Computer Model Results: Premixer Performance	50
5.8 Discussion of Computer Model Results	54
Chapter 6: Conclusions and Recommendations	56
6.1 Conclusions	56
6.2 Recommendations and Future Work	57
References	59

Appendix A: Hydrogen-air Premixer Drawings	61
Appendix B: Airport Lab Hydrogen Supply System Setup	62
Appendix C: CDSL Test Setup Component List	64
Appendix D: Detailed Specifications of the Computer Engine Model	65
Appendix E: Detailed Premixer Operating Conditions at the Flashback Limit	66

List of Figures

Figure 3.1: Solid model of fuel/air premixer, showing inlet (left) and exit (right) ends	9
Figure 3.2: Cross section of the premixer, showing air and hydrogen flow	9
Figure 3.3: Guide vane design showing variation in turning angle from hub to tip.....	10
Figure 3.4: Photo of the unmodified combustor liner	12
Figure 3.5: Photos showing modified combustor liner	13
Figure 4.1: Schematic of the CSDL test setup	15
Figure 4.2: Schematic of the test combustor used in the CSDL Facility	16
Figure 4.3: Photo of the test combustor fitted with the pressure shell	17
Figure 4.4: Premixer operating conditions: combustor pressure versus air flow	18
Figure 4.5: Premixer operating conditions: upstream temperature versus air flow	19
Figure 4.6: Premixer operating conditions: hydrogen mass flow versus air flow	19
Figure 4.7: Gas turbine lab test setup, showing modified engine, dynamometer, and H ₂ supply system	21
Figure 4.8: Modified PT6A-20 hydrogen fuel system layout	22
Figure 4.9: Engine schematic showing installation of premixers and liner	23
Figure 4.10: Custom fabricated combustor liner with premixers installed	24
Figure 4.11: PT6A-20 model setup in GSP	26
Figure 5.1: Photographs showing the operating regimes of the premixer	29
Figure 5.2: Flashback boundary surface for an equivalence ratio of 0.9	31
Figure 5.3: Dependence of flashback mixture velocity on temperature and pressure at equivalence ratios of 0.6, 0.8, and 1.0	33
Figure 5.4: Premixer center body after experiencing flashback	34

Figure 5.5: Plot of compressor outlet pressure versus shaft power for the PT6A-20 operating on Jet-A and hydrogen	36
Figure 5.6: Plot of compressor outlet temperature versus shaft power for the modified and unmodified engine	37
Figure 5.7: Plot of fuel flow versus shaft power for the modified and unmodified engine	38
Figure 5.8: Plot of gas generator speed versus shaft power for the modified and unmodified engine	39
Figure 5.9: Plot of NO _x production versus shaft power for the engine before and after combustor modification	40
Figure 5.10: Plot of actual and predicted compressor outlet pressure versus shaft power for the unmodified engine	42
Figure 5.11: Plot of actual and predicted Jet-A flow versus shaft power for the unmodified engine	43
Figure 5.12: Plot of actual and predicted compressor outlet temperature versus shaft power for the unmodified engine	44
Figure 5.13: Plot of actual and predicted gas generator speed versus shaft power for the unmodified engine	45
Figure 5.14: Plot of predicted air mass flow versus shaft power for the unmodified engine	46
Figure 5.15: Plot of actual and predicted compressor outlet pressure versus shaft power for the modified engine	47
Figure 5.16: Plot of actual and predicted compressor outlet temperature versus shaft power for the modified engine	48
Figure 5.17: Plot of actual and predicted hydrogen flow versus shaft power for the modified engine	49
Figure 5.18: Plot of the predicted air flow versus power for the modified and unmodified engine	50
Figure 5.19: Plot of equivalence ratio and mixture velocity at the premixer exit versus power for a full-power premixer equivalence ratio of 0.4	51

Figure 5.20: Plot of equivalence ratio and mixture velocity at the premixer exit
versus shaft power for a premixer flow split of 20 percent..... 53

Figure 5.21: Plot of actual mixture velocity and flashback mixture velocity versus
shaft power for a premixer flow split of 20 percent 54

Figure B.1: Detailed schematic of the airport lab hydrogen supply system 62

List of Tables

Table 3.1: Table of premixer design operating conditions at three engine conditions	11
Table 4.1: Relevant design point inputs for the GSP engine model	27
Table 5.1: Test conditions where premixer flashback was observed	30
Table B.1: Component list for the airport lab hydrogen supply system	63
Table C.1: List of components used in the CSDL test setup	64
Table D.1: List of component specifications used in the computer engine model	65
Table E.1: List of operating conditions at which premixer flashback was Observed	66

Chapter 1: Introduction

Due to growing concerns about the availability and the combustion emissions associated with fossil fuels, there has been increasing interest in clean, renewable sources of energy. Hydrogen is an attractive fuel for the future for several reasons, the first being that hydrogen can be produced from water using renewable sources such as wind, solar, and geothermal energy. As a result, the potential for hydrogen production is virtually unlimited. Additionally, the emissions concerns associated with hydrogen are considerably less than those associated with fossil fuels. Finally, an increase in the use of hydrogen would mean a reduction of the world's dependence on oil. The focus of the current work is the use of hydrogen as a fuel in a gas turbine engine. Gas turbines are very versatile and reliable, having applications in the air, land, and sea. They have the potential to incorporate hydrogen fuel into a great many applications.

As a gas turbine fuel, hydrogen is attractive because it produces no carbon emissions. This is particularly important in light of growing concerns about continued global warming [1]. In addition to carbon, many fossil fuels produce emissions of sulfur, unburned hydrocarbons, and various other harmful compounds. None of these are associated with hydrogen combustion. However, hydrogen-air combustion may produce one significant type of pollutant also associated with fossil fuels: oxides of nitrogen. Oxides of nitrogen, or NO_x , are a source of smog and acid rain. NO_x is produced through the Zeldovich and Prompt mechanisms when hydrogen is burned in air, with the Zeldovich mechanism being the more significant source [2]. Zeldovich kinetics are highly dependent on temperature and residence time, meaning that more NO_x formation will occur during high residence times at high flame temperatures than during low residence times at lower flame temperatures. In fact, NO_x production is highly nonlinear with flame temperature and NO_x production can be reduced several orders of magnitude by burning at a sufficiently low temperature (below 1700 K) [3].

While several methods exist for lowering the temperatures of hydrogen-air flames, the method that will be the focus of the current work is lean premixed

combustion. In lean premixed combustion, the fuel and oxidizer are mixed at a lean equivalence ratio prior to combustion. The excess air in the reaction acts as a thermal sink, decreasing the temperature of the flame and potentially limiting NO_x to sub-ppm levels [4]. Hydrogen lends itself well to lean premixed combustion due to its wide flammability limits. Hydrogen is flammable at equivalence ratios ranging from 0.1 to 6.8 [5], meaning that it can produce a stable flame under a wide range of conditions. This is a necessity in gas turbine combustion, since conditions vary considerably over the engine's operating range. The design of the hardware associated with lean premixed hydrogen combustion, however, can be challenging. Premixing devices must assure adequate mixing of the fuel and oxidizer while preventing flashback, the potentially damaging upstream propagation of the flame into the premixer.

Premixer flashback has several potential causes. First, insufficient velocities in the boundary layer or bulk flow can allow upstream flame propagation and stabilization. Second, autoignition due to high residence times at high temperatures inside the premixing device can cause flashback. Finally, combustion instabilities can cause a breakdown of the flow field at the premixer exit and upstream flame propagation [6]. These issues are magnified when hydrogen is used as the fuel because of high turbulent flame speeds (as much as 7-8 times those of methane-air flames) [2].

Knowledge of the causes of flashback suggests that a sufficiently high mixture velocity at the exit of the premixer would be a reliable means of preventing upstream flame propagation. Indeed, a very high exit velocity can prevent flashback in hydrogen-air premixers and has relatively little effect on blow-off stability, due to hydrogen's high turbulent burning velocities. Unfortunately, in the context of the current work, a premixer is not a standalone device. It must operate acceptably in a gas turbine combustor, where pressure loss is a significant concern. A premixer designed for excessive exit velocities will create high combustor pressure loss and may cause problems, including decreased cycle efficiency, decreased combustor air flow, decreased compressor surge margin, and high internal temperatures. All of these must be avoided

for lean premixed hydrogen combustion to be a viable technology in gas turbine engines. As a result, designs must strike a balance between flashback resistance and pressure loss.

This paper focuses on a specific premixer design and its application in a modified Pratt & Whitney Canada PT6A-20 turboprop engine. The PT6A-20 is rated at 550 shaft horsepower and comprises a gas generator section and a free power turbine. The engine has been modified to operate using eighteen premixers and a custom-fabricated combustor liner specifically designed to match the premixers. This investigation will examine the design of the premixer and its performance in laboratory tests intended to determine its flashback limits. Additionally, the performance and operability of the modified engine incorporating the premixers will be examined.

Operation of the modified engine was limited to 150 hp during testing due to consistent premixer flashback at this power level. Since premixer flashback was not expected at design conditions, further analysis was required to determine the cause. A computational engine model was created to serve as an analysis tool for engine and premixer operation. The engine model will be used in conjunction with premixer performance data to analyze the interaction between the engine and premixers and to determine the true operating conditions of the premixers in the modified engine. Finally, the model will be used to analyze the potential for engine operation at power levels above 150 hp.

Chapter 2: Review of Literature

The concept of using gaseous hydrogen as a fuel for gas turbines is not new. Several recent examples exist of gas turbines and gas turbine combustors being operated on gaseous hydrogen. One such example is provided by Sampath and Shum [7]. They tested two diffusion nozzle designs—a multi-hole nozzle and a swirl nozzle—in a test combustor representative of gas turbine conditions. The nozzles produced combustion efficiencies as high as 99.95% and good ignition characteristics. However, high flame temperatures led to high combustor wall temperatures and high NO_x levels (up to twice the level produced by Jet-A injected from a simplex nozzle). These results show the advantage of a lean-premixed design which could produce lower flame temperatures, but maintain high combustion efficiency.

Dahl and Suttrop successfully designed and tested a gas turbine combustor that used microdiffusion hydrogen combustion to produce low NO_x levels [4]. In this type of combustor, many small air jets are injected into a low speed hydrogen atmosphere (created by passing hydrogen through a porous metal). The air jets produce flamelets, resulting in a large flame area and a very short residence time of the combustion products at high temperatures. This type of burner is advantageous because it avoids the issue of flashback associated with lean premixed designs. The disadvantage of this burner is that the number of flamelets that can be produced is finite, meaning NO_x levels will not decrease to the level of a premixed flame. Indeed, it is suggested that the NO_x levels produced with this technology are still nearly an order of magnitude larger than those that can be produced in the ideal premixed case.

Brand et al. examined a lean premixed hydrogen-air combustor alongside a lean direct injection combustor [8]. Like Dahl and Suttrop, they found that the premixed combustion scheme had a significantly greater NO_x reduction potential. However, the premixed scheme also presented more stability issues (both blow-off and flashback) than the direct injection scheme. Tests in their lean premixed combustor showed that flashback only occurred during strong transients and was disgorged without damage to

the hardware. This is in contrast to the findings of the present investigation, in which flashbacks can not be disgorged without a shutdown and relight of the premixer. The difference is a result of the premixer geometry and the design of the combustion system used in this investigation. Brand suggested that stability limits can be improved with diffusion piloting to more securely anchor the flame at the premixer exit.

Plee and Mellor compiled an extensive review of recorded flashback events in premixing and prevaporizing devices for gas turbines [6]. They found that the classical flashback mechanism, wherein the burning velocity of the mixture exceeds its actual velocity, either in the boundary layer or in the free stream, is generally not responsible for flashback in these combustors. Instead, flashback is caused by autoignition of the mixture or flame propagation into areas of low velocity or recirculation caused by flow disturbances in the mixing device. Plee and Mellor also suggested the use of equivalence ratio versus combustor loading to define flashback conditions. The combustor loading, $1/\theta$, is defined as follows:

$$\frac{1}{\theta} = \frac{\dot{m}_{air}}{P^{1.75} A_{ref} D_{ref}^{0.75} e^{T \cdot 300}} \quad (2.1)$$

where \dot{m}_{air} is the mass flow rate of the air, P is the combustor pressure, A_{ref} is the combustor area, D_{ref} is the combustor hydraulic diameter, and T is the combustor inlet temperature. The implications of their findings are twofold. First, the geometry of a premixing device can have a more significant effect on tendency toward flashback than the mixture velocity it is designed to produce. Second, the definition of flashback conditions using combustor loading and equivalence ratio may allow laboratory tests of flashback limits to be extended to engine conditions and operation.

Beer and McDonnell investigated the autoignition of hydrogen-air mixtures in conditions representative of those found in fuel/air premixing devices [9]. Ignition delay times were investigated in a turbulent flow at temperatures between 650 and 850 K, pressures between 5 and 7 atm, and equivalence ratios between 0.2 and 0.5. In these tests, autoignition was only found to occur at air temperatures above 750 K and residence times above 100 ms. This suggests that autoignition of the fuel/air mixture is not likely

as a mechanism for flashback in the current investigation, since the expected residence times and inlet temperatures do not support it.

Kröner, Fritz, and Sattelmayer examined the flashback characteristics of a swirl stabilized premixer without a center bluff body [10]. In this type of burner, flashback was found to be caused by combustion induced vortex breakdown (CIVB) at the burner exit. In CIVB, the reacting flow at the mixer exit causes breakdown of the swirling flow and upstream propagation of a recirculation zone into the unburned mixture. This study of flashback revealed that, when this mechanism is responsible, the velocity of the mixture has only a small effect on the equivalence ratio at which flashback occurs. The effect of temperature, however, is relatively large.

Minakawa, Miyajima, and Yuasa designed and tested a non-integral (externally constructed and controlled) lean premixed hydrogen combustor for a micro gas turbine [11]. Tests were performed both in an atmospheric combustor test rig as well as in the combustor/microturbine system. A significant finding of these tests was that flashback occurred in engine operation under conditions that were believed to be safe based on results from the test combustor. Ultimately, flashback in the engine was avoided with changes to the engine starting procedure. The results of these tests reinforce the need to characterize the fuel premixing device as well as the engine itself. A thorough effort to characterize the interaction between the two must be made to assure that a design will be successful.

In summary, a significant volume of work exists on the use of hydrogen as a fuel in gas turbines as well as on the use of hydrogen in lean premixed combustion systems. Gas turbines have been operated successfully using diffusion and microdiffusion hydrogen burners, which produce greater NO_x emissions than lean premixed systems but present no potential for flashback. Tests of lean premixed hydrogen combustors show significant potential for flashback, whose occurrence is strongly dependent on the structure of the premixer flow field. As a result, flashback is difficult to predict and must be examined experimentally. Little work exists on the operability of lean premixed

hydrogen combustors in gas turbines or on the relationship between premixing combustor and engine characteristics. The current investigation specifically addresses these issues associated with the integration of a lean premixed hydrogen combustion system into a gas turbine engine.

Chapter 3: Premixer and Combustor Liner Design

This section describes the design of the hydrogen-air premixer used in the current investigation, as well as the design of the combustor liner installed with the premixers in the modified engine. It is important to note that the investigation of the premixer is specific to the design described here and does not necessarily extend to other geometries. This is because geometry largely determines the stability characteristics and operability of a premixer design. The flashback limit, which is of specific interest in this investigation, has several potential causes that are very dependent on geometry [6]. Similarly, the results of the engine tests apply only to the combustor liner design described here, since the design of the liner strongly affects the premixer operating conditions in the engine.

3.1 Premixer Design

The hydrogen-air premixer design examined here is a slight modification of the design originally presented by Homitz in 2006 [3]. Detailed drawings of the premixer can be found in Appendix A. The premixer design, shown in Figures 3.1 and 3.2, employs swirl and bluff body flame stabilization. Fuel-air premixing is accomplished in an annular channel, where swirl is introduced by four vanes. The vanes are designed to produce a swirl number of 0.6. Swirl number, defined as the ratio of the axial flux of angular momentum to the axial flux of axial momentum, is calculated as follows:

$$S_n = \frac{\int_0^R c_\theta c_z r^2 dr}{R \int_0^R c_z^2 r dr} \quad (3.1)$$

where c is velocity, r is radial distance, and R is the outer radius of the mixing annulus. The subscripts θ and z denote the tangential and axial directions, respectively. A swirl number of 0.6 represents a relatively high level of swirl and is used to assure adequate mixing of the fuel and air [12].

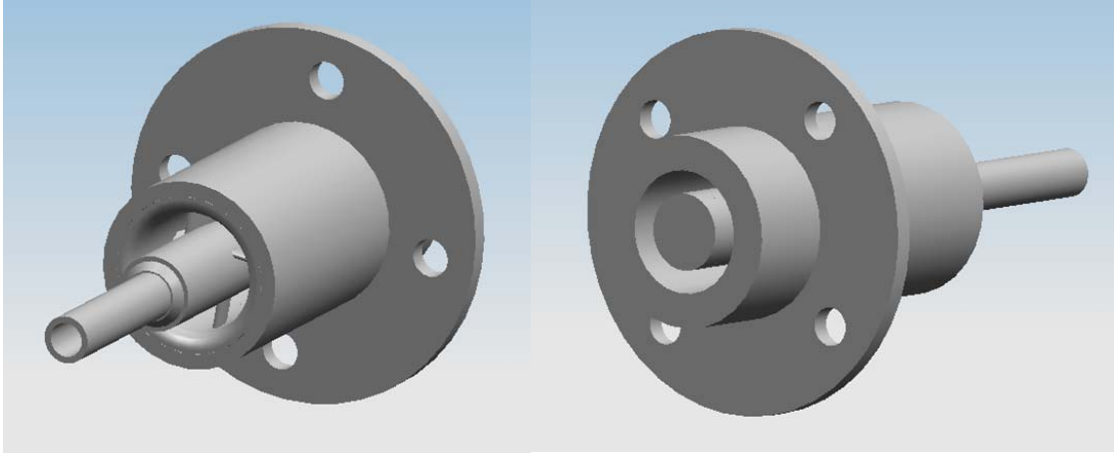


Figure 3.1. Solid model of fuel-air premixer, showing inlet (left) and exit (right) ends.

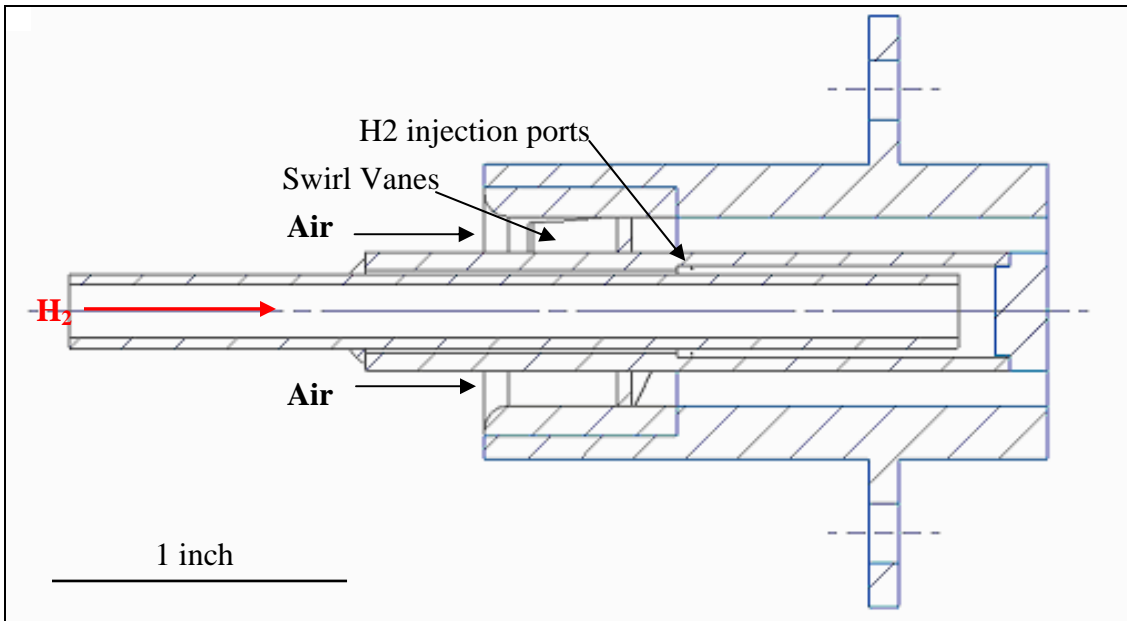


Figure 3.2. Cross section of the premixer, showing air and hydrogen flow.

The swirl vanes used in this premixer design produce 60 degrees of turning at the hub radius and 45 degrees of turning at the tip. The variation in turning angle is a design feature used to produce the radial equilibrium momentum distribution

$$rc_{\theta} = k \quad (3.2)$$

where k is constant. According to the momentum equation,

$$\frac{\partial}{\partial r}(c_z^2) = -\frac{1}{r} \frac{\partial}{\partial r}(rc_{\theta})^2 \quad (3.3)$$

meaning that the specified radial equilibrium condition produces no radial variation in axial momentum. Since there is no radial variation in axial momentum entering the vane passage, the specified radial equilibrium condition should produce the smallest total pressure loss [13]. The design of the guide vanes accounts for the only significant difference between the premixer of the current investigation and the one designed by Homitz. In Homitz' design, a twisted vane geometry was used to achieve the required radial variation in tangential velocity. The vanes were prohibitively difficult to manufacture, leading to the current design, which uses a constant radius vane. Shown in Figure 3.3, the revised vane uses a spanwise variation in chord length to achieve the desired tangential velocity distribution.

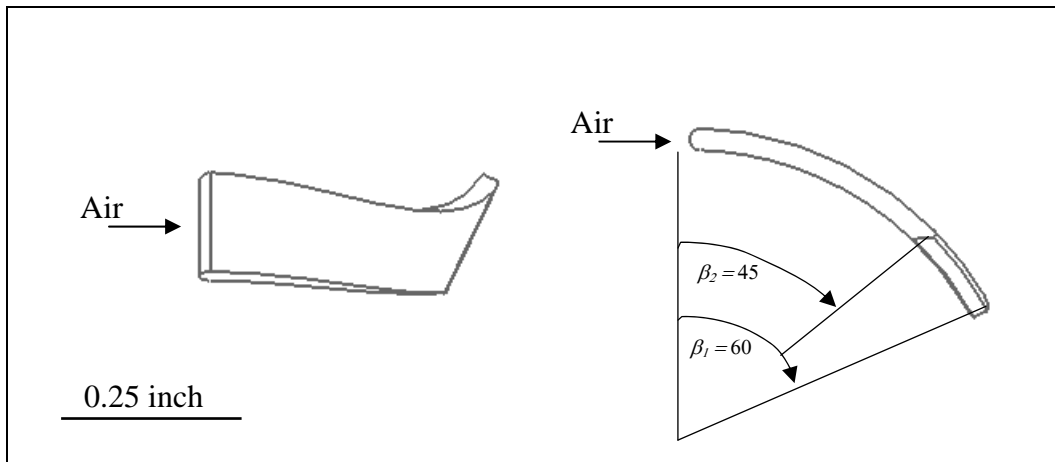


Figure 3.3. Guide vane design showing variation in turning angle from hub to tip

In the current design, hydrogen is injected through eight injection ports just downstream of the vanes. Prior to injection, the fuel passes over the inner wall of the bluff body to provide cooling. Each injection port has a diameter of 0.013 inches, representing a small change from Homitz' design, which called for a port diameter of 0.01 inches. The change was made to improve manufacturability while maintaining the requirement that the fuel jets be choked during operation. The choked fuel jets provide good penetration into the main flow and eliminate the potential for combustor pressure variations to affect the fuel flow rate. It should be noted that the fuel jets are placed as far as possible out of the vane wakes to prevent flame stabilization in the low-velocity regions.

The premixer used in this investigation was designed to perform over a wide operating range. Table 3.1 shows the operating conditions for the premixer at several engine operating points. The conditions shown are for one premixer operating in the combustor of the engine at the design equivalence ratio of 0.4. According to the literature [3], a design equivalence ratio of 0.4 would ideally limit flame temperatures to less than 1700 K and NO_x to sub-ppm levels. The Jet-A flow requirements of the unmodified engine were used to determine the energy equivalent hydrogen flow (based on LHV) at each point and the equivalence ratio determined the required air flow. High exit mixture velocities are a feature of the design intended to inhibit flashback. However, low equivalence ratio stability is still possible at these velocities due to strong bluff body flame stabilization and the high burning velocity of hydrogen. The importance of wide stability limits is reinforced when it is noted that the equivalence ratio of the premixers inside the engine is likely to vary considerably from the design value of 0.4 over the engine's operating range. This will be investigated further in later chapters.

Table 3.1. Table of premixer design operating conditions at three engine conditions.

Engine Operating Point		Premixer Operating Conditions				
Condition	Power Level (hp)	Pressure (atm)	Inlet Temperature (C)	Air Flow (g/s)	Fuel Flow (g/s)	Mean Mixture Velocity (m/s)
Idle	~5	1.56	88.1	19.8	0.23	119
Cruise	450	5.10	227	80.8	0.95	208
Full Power	550	5.57	249	98.2	1.15	241

3.2 Combustor Liner Design

As stated, the design of the combustor liner largely determines the operating conditions experienced by the premixers in the modified engine. Specifically, the pressure-flow characteristic of the combustor liner determines the fraction of the compressor discharge air that passes through the premixers and the fraction that provides cooling and downstream dilution. The combustor liner used in the current investigation is a heavily modified version of the liner used in the unmodified engine, shown in Figure

3.4. Since the combustor of the unmodified engine relied on diffusion burning, the air flow through the original liner went entirely to dilution of the combustion products and film cooling of the liner wall.

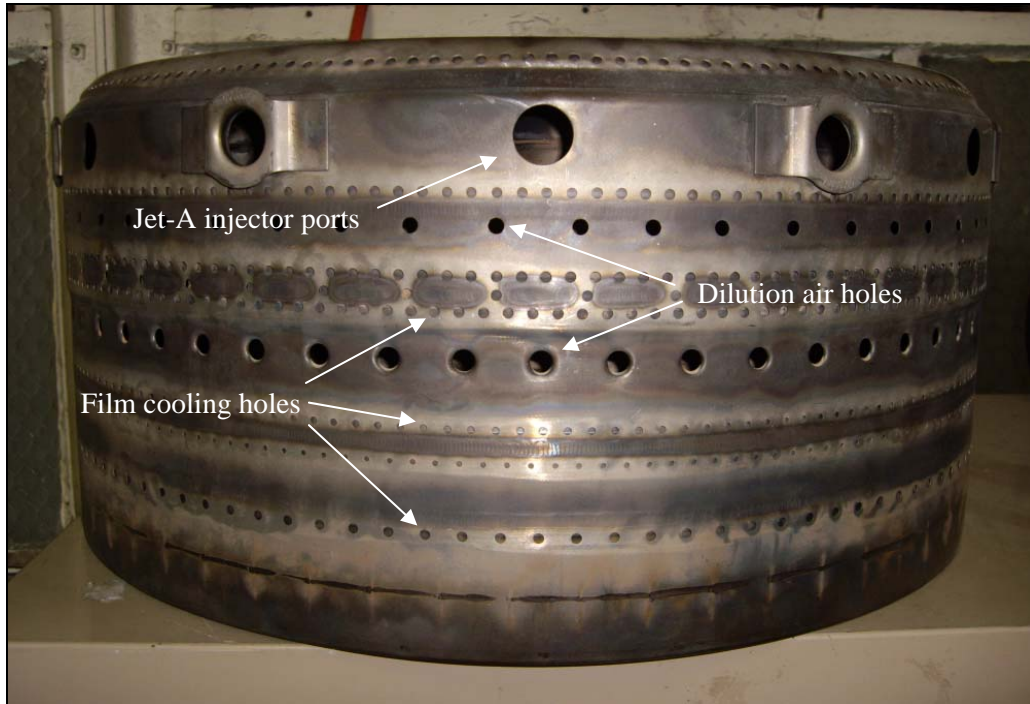


Figure 3.4. Photo of the unmodified combustor liner

To allow successful operation of the premixers in the engine, the combustor liner was modified, as shown in Figure 3.5. The length of the liner was decreased to approximately one third the length of the unmodified liner to provide space in the gas generator case for the premixers. The premixers were affixed to a flat plate containing 18 holes, which was welded on the upstream end of the liner. The film cooling incorporated in the downstream portion of the original liner was left in tact, while a set of large dilution holes near the premixer exits were covered to avoid affecting flame stability. Finally, additional dilution air holes were added to the modified liner, both in the upstream flat plate (producing a flow parallel to the premixer flow) and in the extreme downstream region of the combustor's outer wall (perpendicular to the premixer flow).

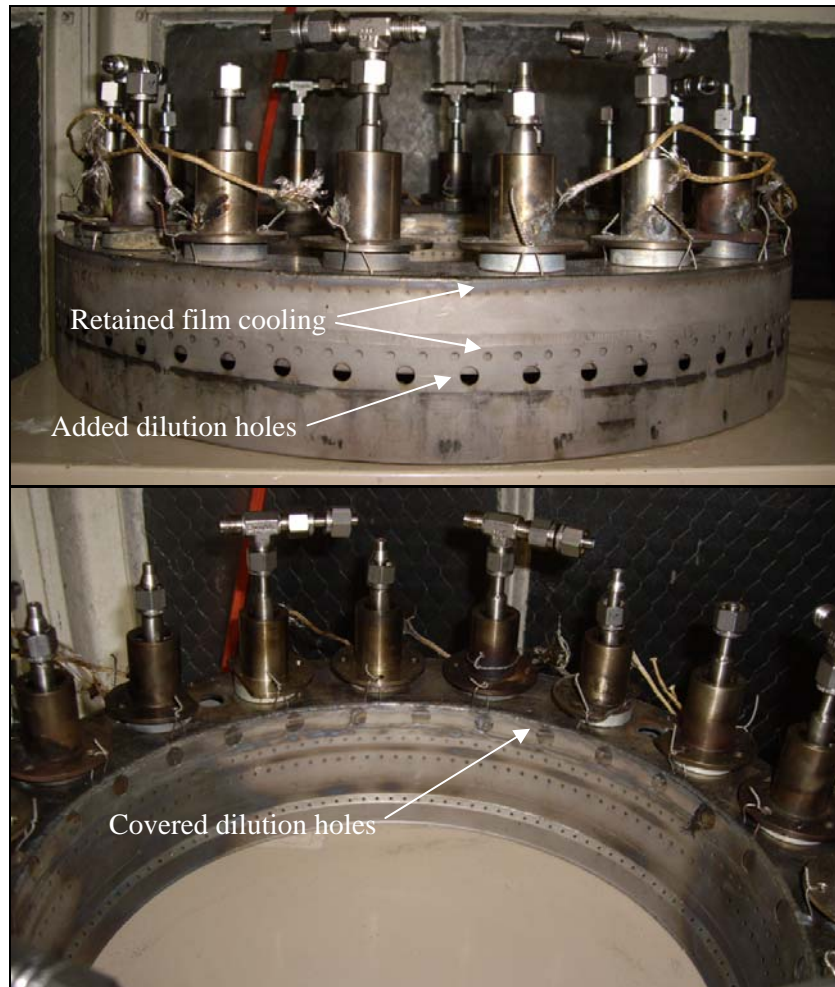


Figure 3.5. Photos showing modified combustor liner

Since the design of the combustor liner strongly influences the premixer airflow, particular attention was paid to the amount of dilution air area incorporated into the modified liner. The liner was designed to pass 65 percent of the compressor discharge air through the premixers and 35 percent through dilution and film cooling, resulting in a premixer equivalence ratio of 0.4 at full power conditions. This was accomplished by first examining the atmospheric pressure-flow characteristics of the premixer as well as the modified liner prior to the addition of dilution cooling. Liner air flow was assumed to scale linearly with the total area of the film cooling and dilution holes. Thus, the area of the dilution holes added corresponded to the area increase that resulted in the desired 65/35 premixer/liner flow split at a given relative pressure loss. It will be shown later that the success of this design strategy was relatively poor.

Chapter 4: Research Plan

This section outlines the process that was used to evaluate and model the operation of the hydrogen-air premixer in the combustion laboratory and in the modified engine. First, the test setup and test strategy used at the Combustion Systems Dynamics Lab (CDSL) to determine the premixer performance will be discussed. This is followed by a discussion of the engine test setup at the Gas Turbine Laboratory and the tests performed to determine engine performance and operability after modification with the premixers. Finally, the strategy for the creation of a computer model to predict engine and premixer performance will be discussed.

4.1 Combustion Lab Test Setup

Premixer performance tests were carried out at the Virginia Tech Combustion Systems Dynamics Lab (CSDL). The facility, shown schematically in Figure 4.1, allows complete characterization and testing of the premixer through full independent control of fuel flow, air flow, temperature, and pressure. In this test setup, up to 0.7 kg/s of dry air is supplied by a compressor and air dryer. The compressed air enters the system at 10 atm, where its pressure is initially reduced by a globe valve. The air passes through a flow meter and a second globe valve is used to control the mass flow rate. The metered air passes through an electric heater capable of delivering up to 300 kW of heat to the system. The heated air then enters the test section, where it flows through the combustor housing the premixer. The premixer receives metered fuel from the fuel system, which uses a pressure regulator to control the flow of hydrogen from the hydrogen supply tanks. After combustion in the test section, the combustion products flow into the cooling section, where a water spray decreases their temperature. The gases then flow through a back pressure valve, which is used to set the pressure in the test section. Finally, the gases are exhausted to the atmosphere.

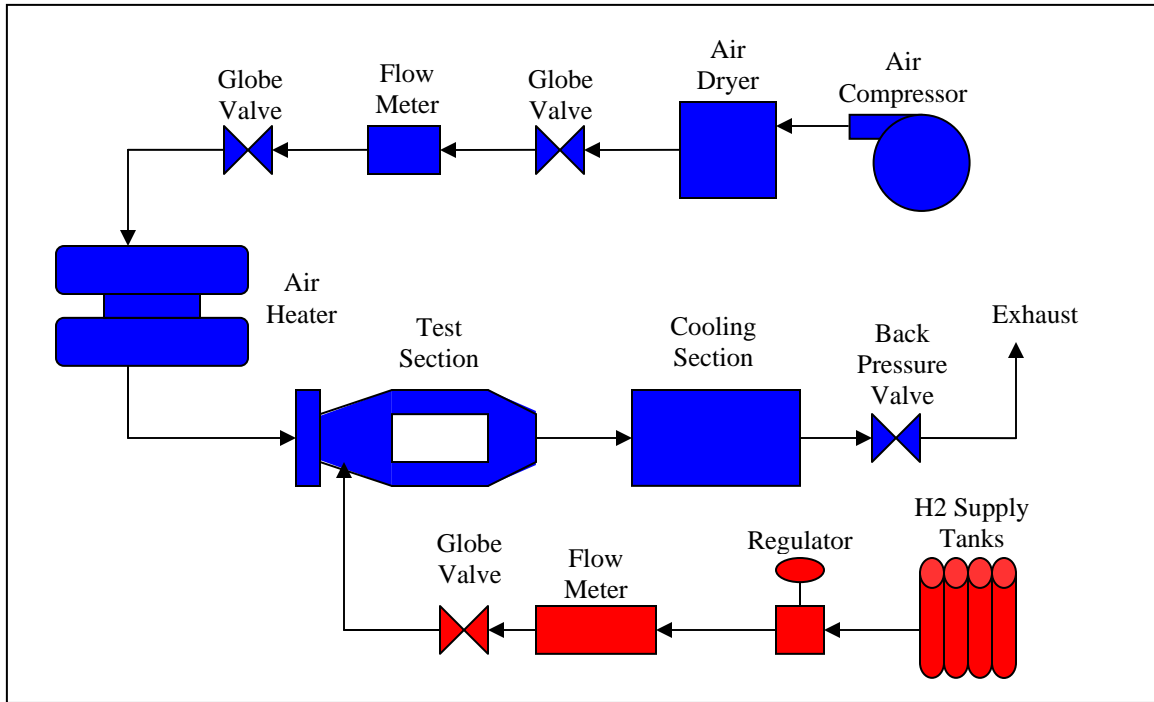


Figure 4.1. Schematic of the CSDL test setup

The combustor used in the premixer performance tests is shown schematically in Figure 4.2. In the test combustor, the premixer receives air from an upstream plenum and fuel from an external fuel supply line. The premixer is inserted into a bulkhead that separates the upstream plenum from the downstream combustion region. The bulkhead seals in channels containing graphite gaskets on the side panels and bolts to the upper and lower walls of the combustor. This eliminates leaks, which can cause inaccurate premixer air flow measurements. A pair of dilution air manifolds are fabricated integral with the bulkhead. These manifolds receive metered external high pressure air, which is dispersed to the downstream side of the bulkhead. The additional cool air protects the combustor from hot combustion gases, particularly at high premixer equivalence ratios. A viewing window in one side panel allows the flame to be visually analyzed, while a thermocouple mounted on the premixer's outside shell allows its temperature to be monitored.

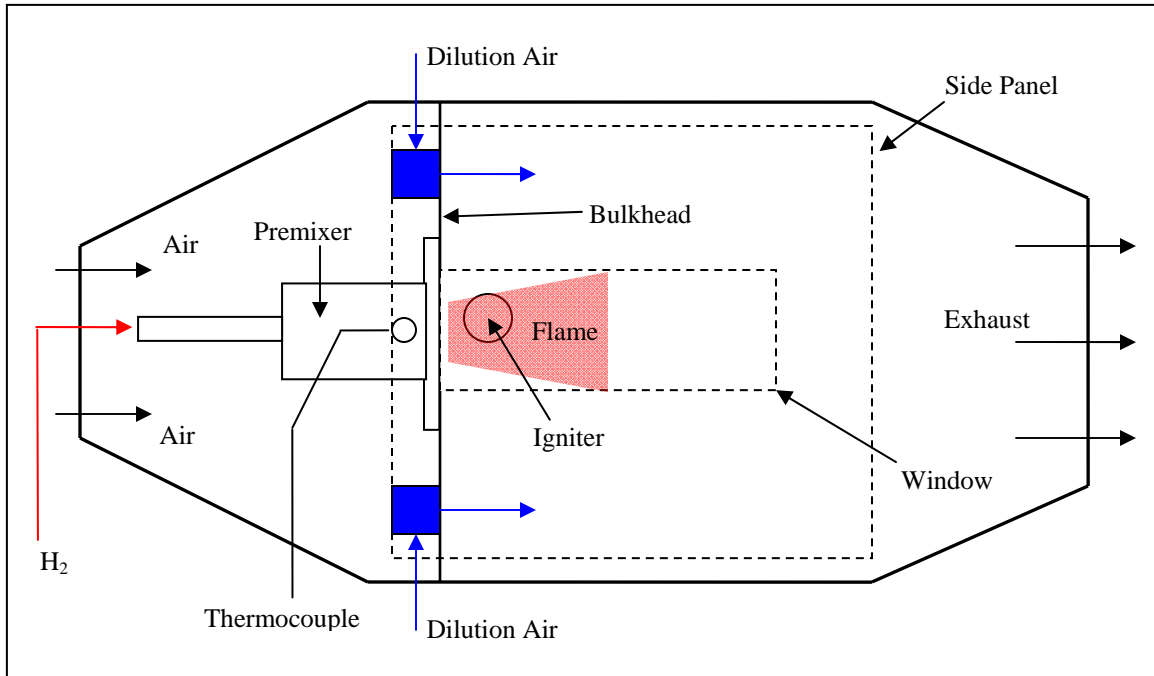


Figure 4.2. Schematic of the test combustor used in the CSDL facility.

For the premixer stability tests, the combustor was encased in a pressure shell, as shown in Figure 4.3. The pressure shell allowed the combustor pressure to be raised above atmospheric to accurately reproduce the conditions produced by the engine. Additional dilution air lines flow cool (unheated) air into the pressure shell outside of the combustor, aiding in combustor and post-combustor cooling and providing additional control of the combustor back pressure. The viewing window in the pressure shell aligns with the window in the combustor to provide a line of sight to the flame.

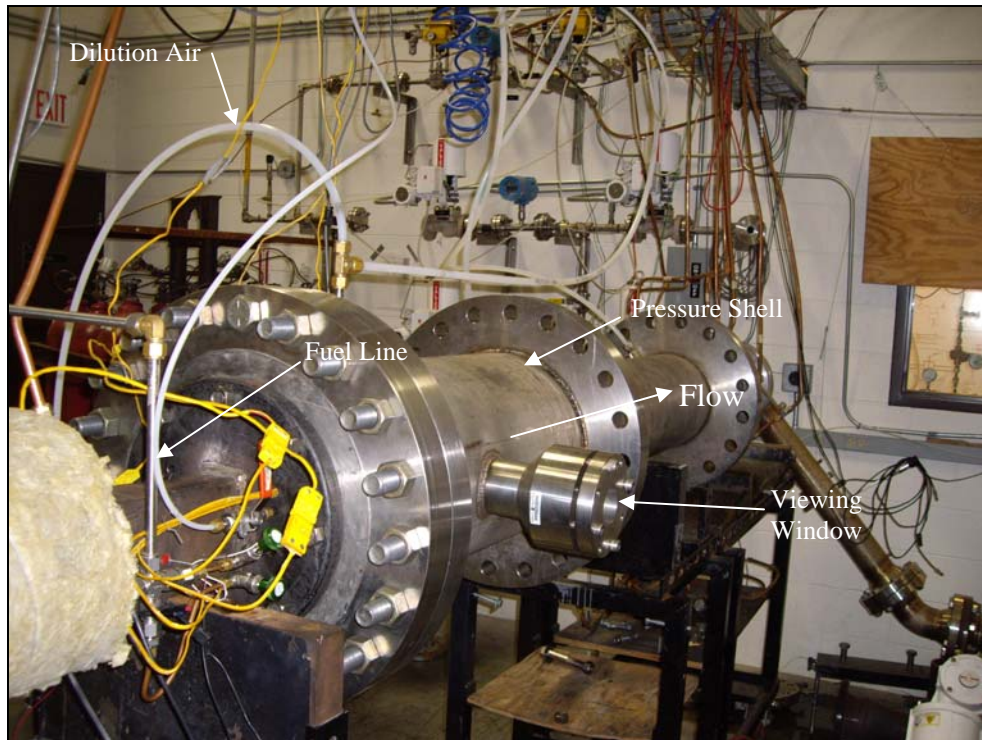


Figure 4.3. Photo of the test combustor fitted with the pressure shell.

4.2 Combustion Lab Test Strategy

Due to the results of work performed by the research team prior to this investigation, the flashback limits of the premixer were of particular importance in the CSDL tests. As confirmed by the literature review, the flashback phenomenon is influenced by many factors, related both to the flame and the premixer flow field. Indeed, the potential for premixer flashback stems from flow field features which are produced by the premixer geometry [6]. However, for a flashback to occur, the turbulent burning velocity must exceed the unburned mixture velocity, even if only in a localized region of the premixer flow field. It is of great importance, then, to consider factors which affect burning velocity. These factors include pressure, temperature, turbulence intensity, and fuel/air equivalence ratio [2]. Pressure, temperature, and equivalence ratio can be controlled in the CSDL test setup. Turbulence intensity cannot be controlled, except by combustor modifications (e.g. the addition of screens), and is difficult to

measure. However, prior tests of the premixer showed that the upstream flow field had little effect on the combustion characteristics, indicating that the turbulence produced within the premixer was the dominant factor. Turbulence intensity, then, can be considered a result of the premixer geometry and not a controllable test condition.

While virtually limitless combinations of pressure, temperature, equivalence ratio, and mixture velocity can be produced in the test combustor, only specific operating conditions are of interest. These conditions correspond to those which could be encountered in the modified engine. A test plan, then, was developed based on data taken during tests of the unmodified PT6A-20. Figures 4.4 through 4.6 show the combustor pressure, temperature, and hydrogen fuel flow (based on Jet-A energy equivalence) versus the premixer air flow required to achieve the design equivalence ratio of 0.4.

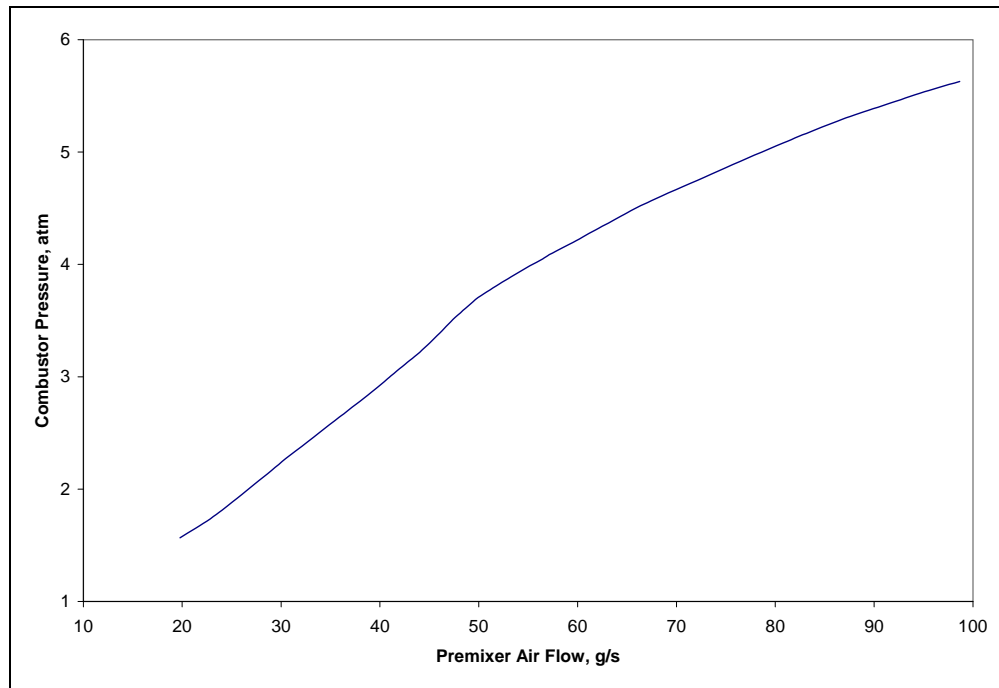


Figure 4.4. Premixer operating conditions: combustor pressure versus air flow.

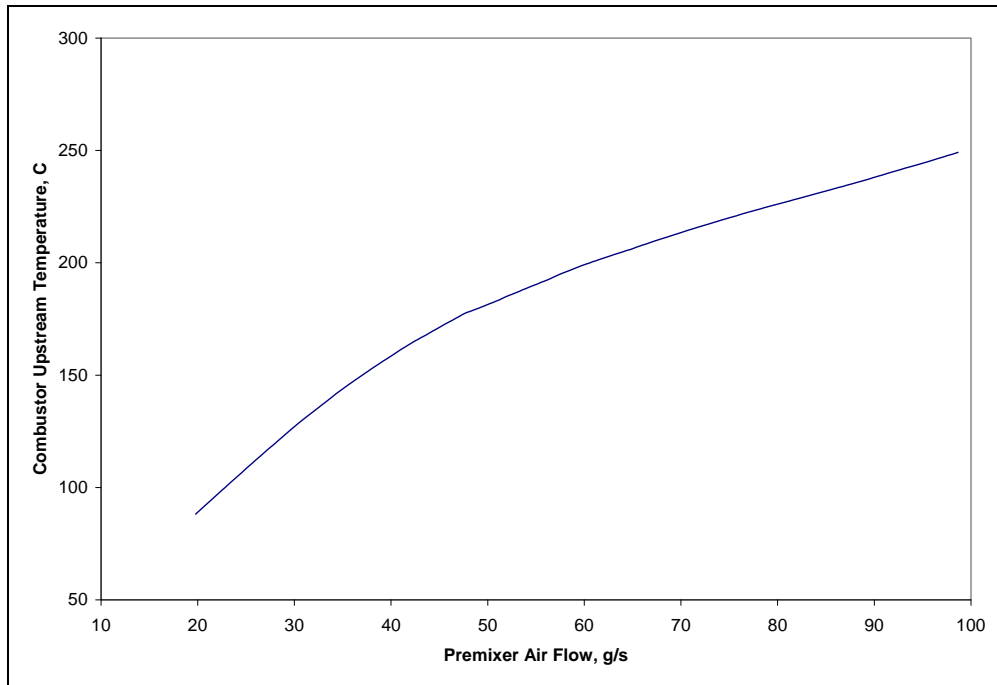


Figure 4.5. Premixer operating conditions: upstream temperature versus air flow.

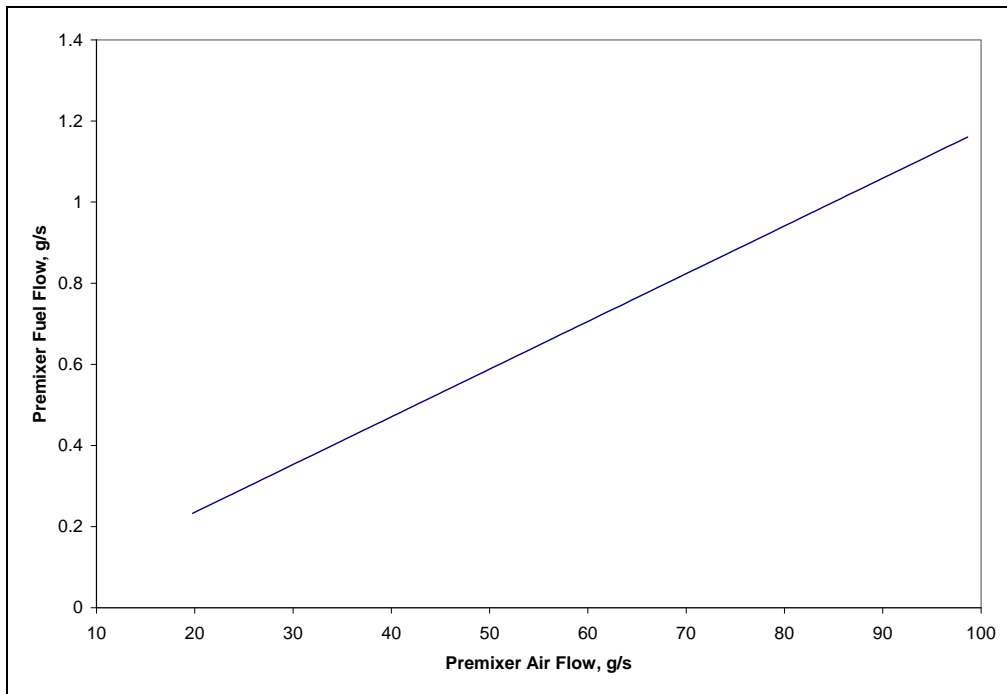


Figure 4.6. Premixer operating conditions: hydrogen mass flow versus air flow.

Since the test plan required the determination of unknown premixer operating limits, a test matrix of specific operating points was not created. Instead, an air flow rate

and the corresponding operating conditions shown in Figures 4.4 through 4.6 were first established in the test setup. Once a design operating point had been reached, the air flow rate was decreased and the pressure and temperature held constant. This resulted in a simultaneous increase in equivalence ratio and decrease in mixture velocity. The procedure was performed repeatedly, starting at points along the operating line and terminating when premixer flashback occurred.

The selected test strategy was appropriate, because combustor pressure and fuel flow did not vary considerably from the original operating line after modification of the engine (this was shown in tests of the modified engine). Premixer air flow, however, is dependent both on the engine operating line and the flow split created by the combustor liner. This makes premixer air flow the only parameter not effectively fixed by the characteristics of the engine. It should be noted that control over the inlet air temperature was relatively coarse, due to long transients associated with the heating system. As a result, temperatures during the tests were not always accurate with respect to the design operating line.

Once a collection of points at which flashback occurred were recorded, a mathematical expression for the flashback limit could be created. The mixture velocity at flashback, u_F , was assumed to have the following dependence:

$$u_F = f(P, T, \phi) \quad (4.1)$$

where P is the combustor pressure, T is the combustor inlet temperature, and ϕ is equivalence ratio. Pressure, temperature, and equivalence ratio were chosen as the independent variables because, as previously discussed, they affect burning velocity and are controllable in the test setup. An empirical expression for the dependence in equation 4.1 will give the operating limits for the premixer and, as will be shown, can provide insight into the operation of the premixer in the modified engine.

4.3 Gas Turbine Lab Test Setup

The modified Pratt and Whitney Canada PT6A-20 test setup is housed in the Gas Turbine Laboratory at the Virginia Tech Montgomery Executive airport. Figure 4.7 is a photograph of the test setup. The engine test stand utilizes a water brake dynamometer capable of dissipating up to 1,000 hp. The dynamometer uses a PID control to vary the load on the engine's output shaft, holding its speed at a preset level. In the current setup, the speed of the output shaft is held constant at 2,000 rpm. A load cell measures the torque applied to the output shaft.

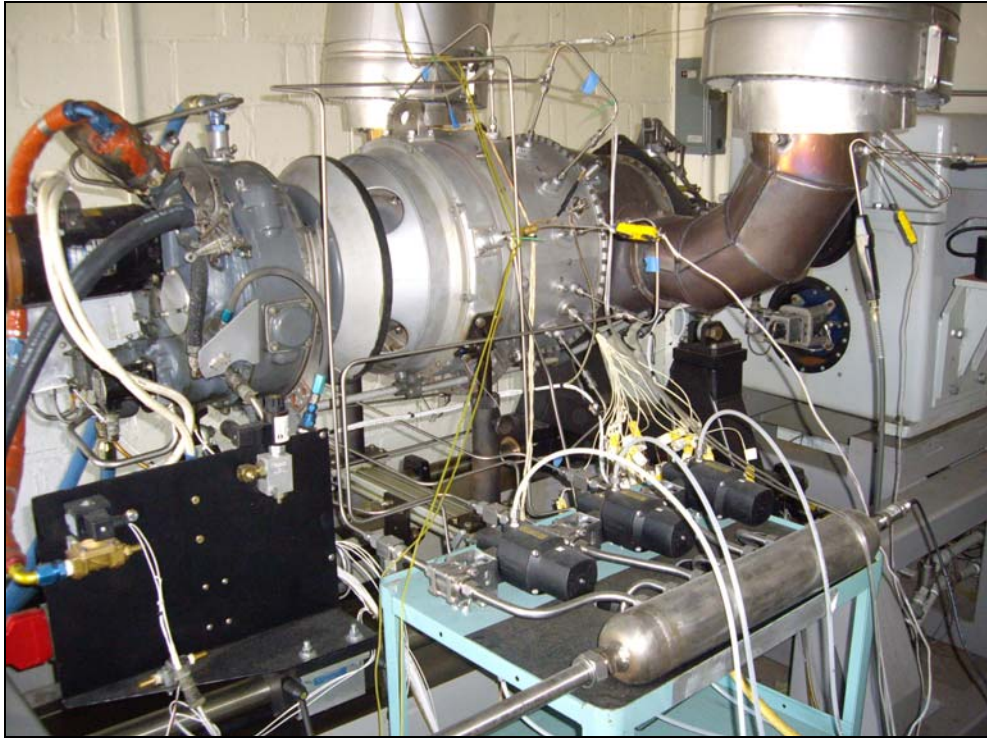


Figure 4.7. Gas turbine lab test setup, showing modified engine, dynamometer, and H₂ supply system.

Figure 4.8 is a schematic of the hydrogen supply system used with the modified engine. Hydrogen is supplied at 2,300 psig from a set of storage tanks totaling 3,000 scf. Immediately downstream of the supply, a regulator decreases the fuel pressure to 800 psig and pneumatically actuated valves distribute the fuel throughout the system. Once the fuel enters the test cell plumbing, its pressure is decreased to the engine operating

pressure. This pressure is set by an electronically controlled regulator and, due to the premixers' choked fuel injection ports, provides direct control of the fuel flow rate into the engine. Fuel flow is measured by a turbine type flow meter.

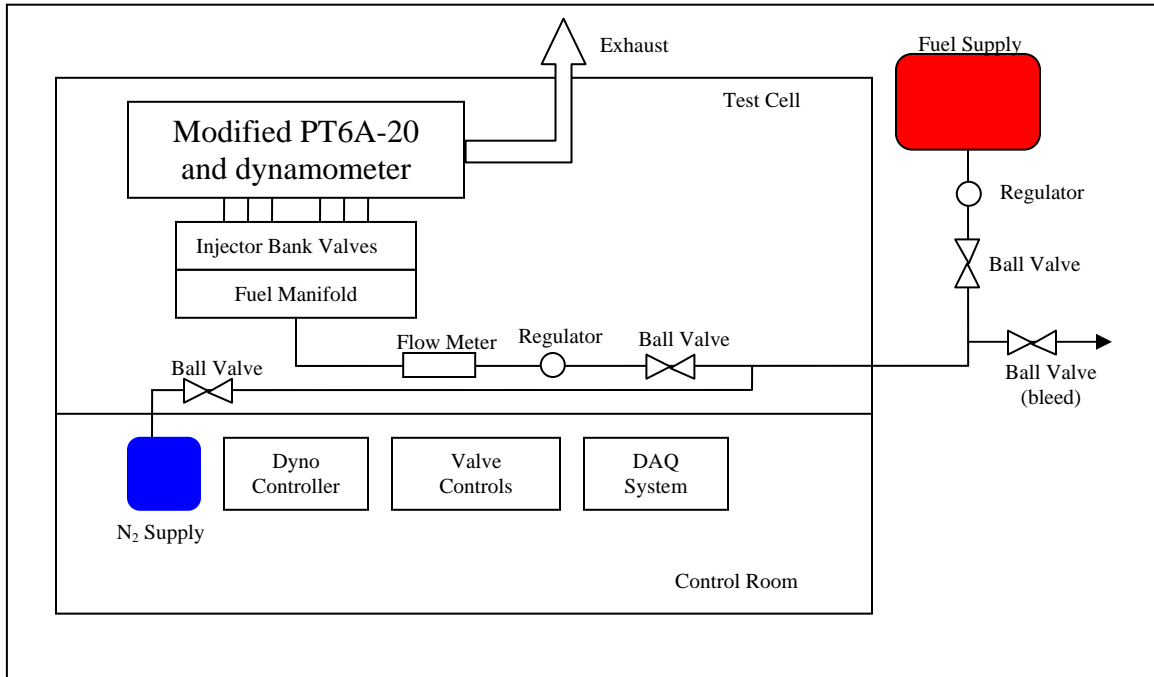


Figure 4.8. Modified PT6A-20 hydrogen fuel system layout.

The engine contains 18 premixers, arranged in six banks of three. The number of premixers was selected early in the design process and was chosen to provide a compact flame and an even temperature distribution at the compressor turbine inlet [3]. Each bank of three premixers is connected to a pneumatic shutoff valve, allowing for staged starting, as well as the deactivation of sets of premixers in the event of a flashback. The shutoff valves and all system valves are controlled by a set of electronic solenoid valves located in the control room. The system incorporates a nitrogen purge, as well as a secondary regulator which provides idle fuel flow in the event of a failure of the electronic regulator. Finally, a CO₂ fire suppression system can flood the test cell in case of a fire.

The premixers were installed in the engine as shown in Figure 4.9. The annular combustor liner, shown in Figure 4.10, was custom fabricated to match the pressure-flow characteristics of the premixers and designed to provide the correct flow split to achieve

the design equivalence ratio. Tests showed, however, that the flow split between the premixers and liner was not as designed. A secondary goal of the investigation thus became the determination of the actual value of the flow split and to examine its implications for engine and premixer performance.

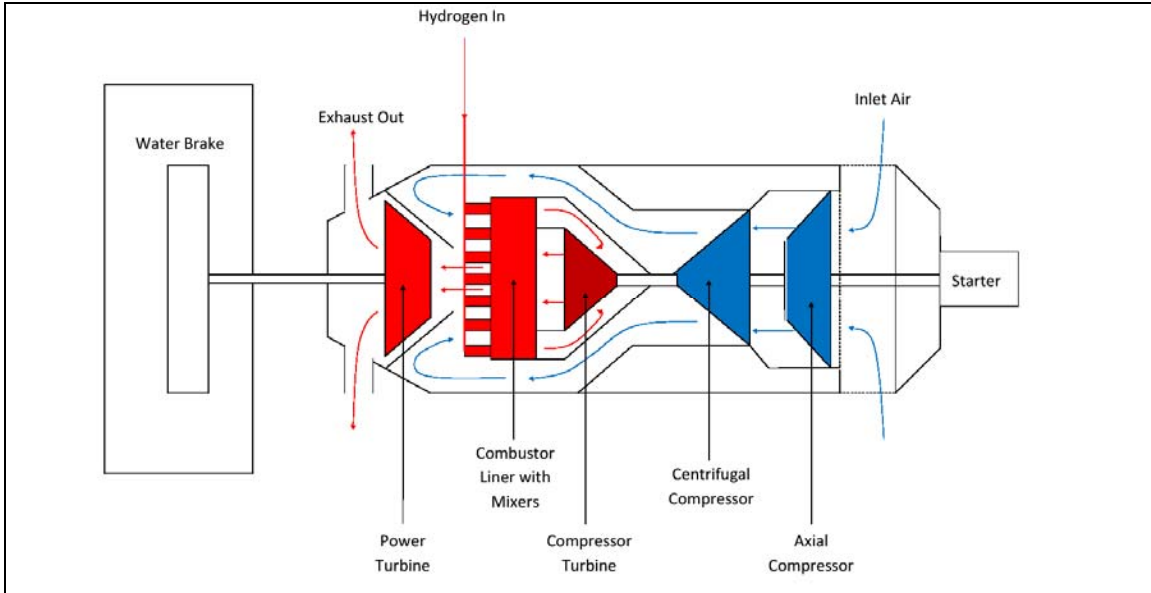


Figure 4.9. Engine schematic showing installation of premixers and liner

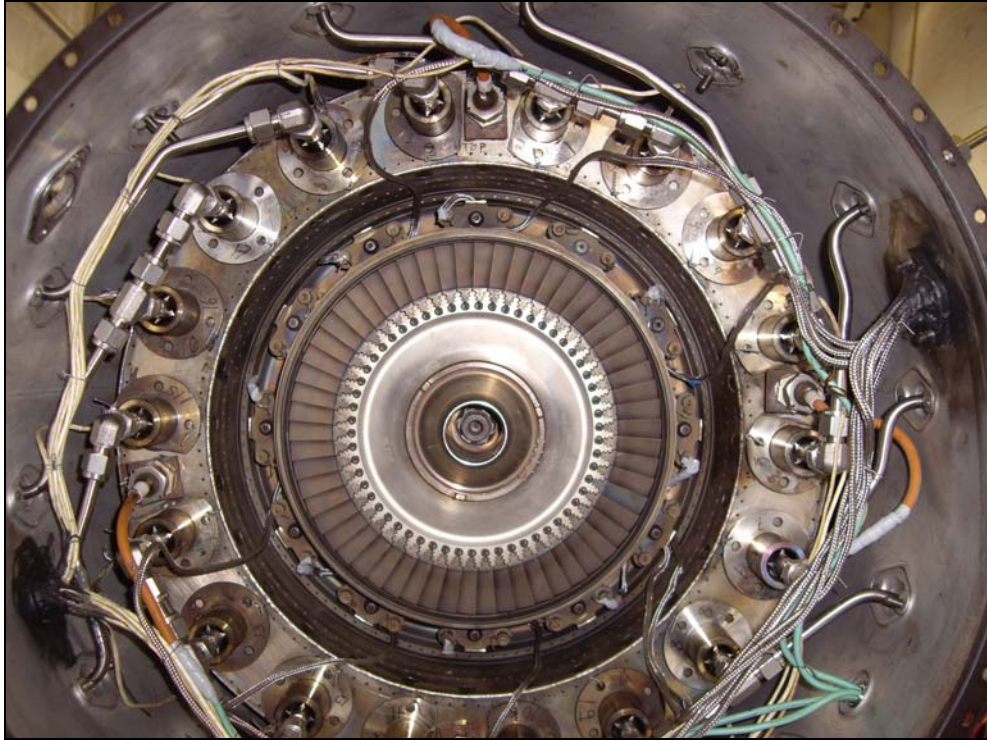


Figure 4.10. Custom fabricated combustor liner with premixers installed.

4.4 Engine Test Strategy

Tests of the premixers in the modified PT6A-20 are considerably more constrained than tests at the CSDL facility. As was shown by the data plotted in section 4.2, the engine operates on a specific linked schedule of fuel flow, air flow, temperature, and pressure. This schedule is not easily influenced, making the combustor liner design and corresponding liner/premixer flow split the only significant control over the premixer operating conditions in the engine. This, along with the fact that premixer operating conditions can be affected in transient operation, dictates the operating procedures for the engine. In contrast to the CSDL tests, which examined the operating limits of the premixers, the engine tests examined the effects of the premixers on the operating limits of the engine.

For our tests, engine operation between light-off and idle was performed in a staged manner. First, the starter was engaged, driving the gas generator at approximately 18 percent N_g . A fuel pressure was then set to achieve the desired light-off conditions. Experience showed that a fuel pressure of 50 psig was appropriate. With the fuel pressure set, the igniters were activated and banks of premixers were opened in succession, separated by the time necessary to observe a rise in inter-turbine temperature (ITT). After all pre-mixer banks were lit, the fuel pressure was increased until idle operation was achieved. Idle operation was considered to be the observed minimum in ITT, which occurred at approximately 62 percent N_g . While self-sustaining operation occurred at a somewhat lower gas generator speed, the specified idle speed was considered to be safer. The igniters and starter were deactivated after idle was achieved and idle operation was maintained for two minutes to allow the engine and premixers to achieve thermal equilibrium.

After the idle period, the fuel pressure was increased slowly to achieve a desired power level. A slow increase in fuel pressure produced quasi-steady operation and avoided transient increases in local equivalence ratio and combustor pressure that could lead to pre-mixer flashback or compressor stall. When a desired power level was achieved, two minutes of steady operation was sustained to again allow thermal equilibrium. Power was then reduced to the idle level and the engine shut down by closing the fuel valves on the pre-mixer banks. Operation on the starter cooled the engine and premixers after shutdown. If, at any time during operation, a transient increase in equivalence ratio or a steady operating condition caused a flashback in one or more premixers, the corresponding pre-mixer bank was shut down and the power level returned to the idle condition. At the idle condition, the re-light of the affected premixers was shown to be safe.

4.5 Computational Engine Model

As will be shown in later sections, the tests of the modified engine proved the need for a model that accurately predicted its performance under a variety of conditions

and could be used to evaluate pre-mixer operability. The software chosen to model the engine was NLR's (Nationaal Lucht- en Ruimtevaartlaboratorium – National Research Laboratory) Gas turbine Simulation Program (GSP) [14]. The program allows a model to be assembled from a library of standard components with performance based on user defined design point inputs. A library of standard component maps can be scaled to the design point and used to predict off-design behavior. Figure 4.11 shows the GSP model of the PT6A-20. The model incorporates the major physical components of the engine, including the inlet, compressor, combustor, compressor turbine, free power turbine, and exhaust duct. Three additional components—the bleed control, fuel control, and load control—are used by the software to provide control inputs to the model.

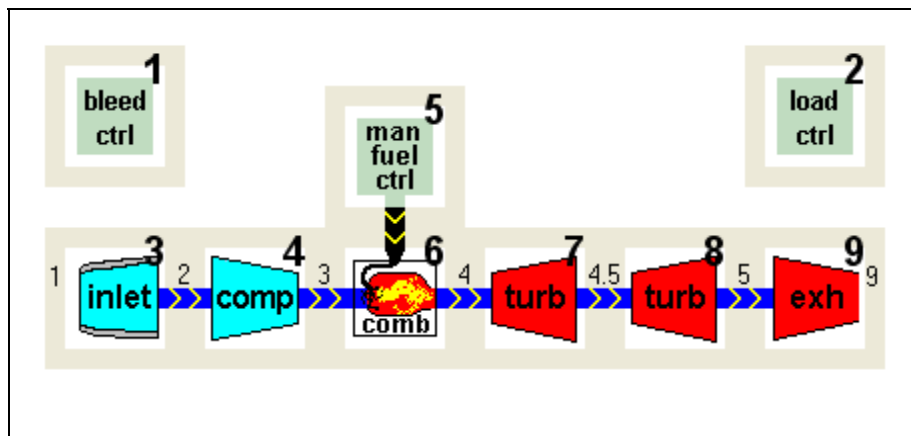


Figure 4.11. PT6A-20 model setup in GSP.

The design point inputs for the components used in the GSP engine model are listed in Table 4.1. The fuel flow, air flow, rotor speeds, and power output are based on the manufacturer's specifications of the engine's full power performance. While the compressor pressure ratio is specified by the manufacturer as 6.2, a pressure ratio of 5.9 has been found to more accurately represent the full power performance of the unmodified test engine. Component characteristics that were not specified by the manufacturer (e.g. compressor and turbine isentropic efficiencies) were estimated from typical values and unmodified engine performance data. It should be noted that the specified combustor dry pressure drop of 2.0 percent is significantly lower than typical values, which range between four and six percent [13]. This pressure drop has been

estimated based on Pratt and Whitney Canada’s specifications and is supported by the literature [7]. Design point specifications not listed in the table are included in Appendix D.

Table 4.1. Relevant design point inputs for the GSP engine model.

Component	Parameter	Value
Inlet	Air mass flow rate	2.95 kg/s
	Pressure ratio	0.988
Compressor	Rotor speed	38,100 rpm
	Pressure ratio	5.9
	Isentropic efficiency	0.812
Combustor	Fuel flow (Jet-A)	0.0585 kg/s
	Combustion efficiency	0.95
	Relative pressure loss	0.02
Compressor Turbine	Rotor speed	38,100 rpm
	Isentropic efficiency	0.85
Power Turbine	Rotor speed	33,000 rpm
	Isentropic efficiency	0.72
Exhaust Nozzle	CD	1.0
Bleed Control	Bleed Schedule	Linear decrease from 20% to 0% between 5 and 150 hp

Chapter 5: Experimental and Computational Results

This section presents the results of the CSDL premixer tests and modified engine tests, as well as the model analysis. First, the observed flashback limits and the empirical model of the mixture velocity at flashback are examined. Second, the results of the modified engine tests, including the observed operating limits, are presented. Finally, the predictions of the engine model as they relate to the engine as well as the premixer performance are discussed.

5.1 Results of the Premixer Tests

The CSDL tests examined the flashback limits of the premixer at fuel flows, pressures, and temperatures that are possible along the engine's operating line. Tests were started at an equivalence ratio of approximately 0.4 and the air flow was subsequently slowly decreased while the combustor pressure was held constant. As the air flow was decreased, the shape of the flame changed as shown in Figure 5.1 (the premixer shell and center body locations are indicated on the left of the photos). When operating near design conditions (shown in a), the flame stabilized on the premixer center body only and extended approximately one inch downstream. A large region of unburned mixture was visible between the premixer exit and the flame. As the air flow was decreased, the flame stabilized on the outer shell of the premixer as well as the center body and elongated considerably (shown in b). The region of unburned mixture at the outlet of the annulus was still visible, but was significantly smaller than at design conditions. Finally, at a sufficiently low mixture velocity, the flame detached abruptly from the bluff body and stabilized entirely within the annulus (shown in c). This behavior signified a flashback and produced a significant rise in the premixer temperature. Immediately after the occurrence of a flashback, the fuel flow was stopped and the test reset to a new operating condition.

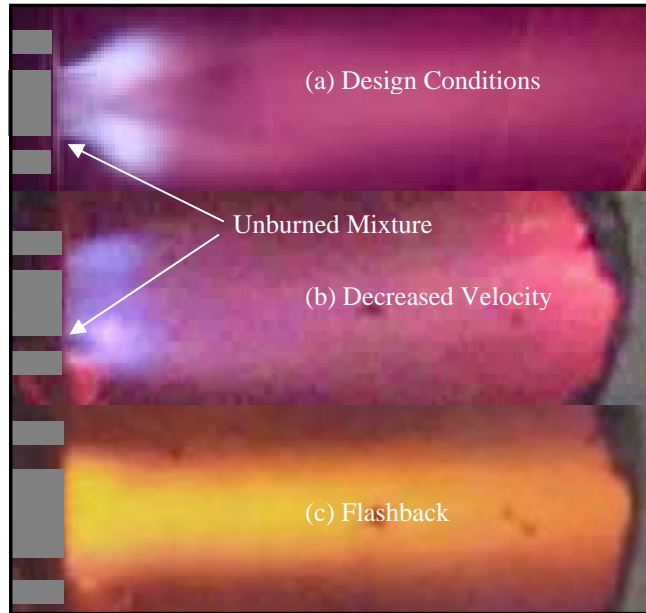


Figure 5.1. Photographs showing the operating regimes of the premixer.

Table 5.1 shows the combinations of pressure, temperature, and equivalence ratio where flashbacks were produced during the tests, as well as the corresponding axial mixture velocities at the premixer exit when the flashbacks occurred. It should be noted that tests at pressures below 2.6 atm did not produce flashbacks. This is primarily due to limitations of the test setup, which prevented the establishment of a sufficiently low air flow rate to produce flashback at low-pressure conditions. Similarly, flashbacks were not observed at equivalence ratios below 0.6. In fact, most flashbacks occurred in the equivalence ratio range between 0.8 and 1.0. Again, the inability to attain sufficiently low mixture velocities prevented the observation of flashback at lower equivalence ratios. Finally, flashbacks could not be produced during tests where the inlet air was unheated. A separate phenomenon, in which fuel propagated upstream and ignited in the plenum area was observed at very low air flow rates. However, the conditions required to support this phenomenon are essentially unattainable in the engine and the data are not included in this discussion.

Table 5.1. Test conditions where premixer flashback was observed.

Upstream Pressure (atm)	Air Temperature (C)	Equivalence Ratio	Mixture Velocity (m/s)
2.62	133	0.775	63.2
2.79	105	0.750	59.8
3.09	58	0.735	44.5
3.10	130	0.802	60.8
3.11	69	0.786	51.0
3.13	141	0.876	65.2
3.14	62	0.867	52.5
3.32	89	0.851	55.8
3.34	104	0.854	56.3
3.45	132	0.937	60.3
3.45	149	1.002	68.5
3.47	74	0.759	57.8
3.48	145	0.607	72.5
3.59	140	0.854	68.1
3.59	108	0.805	66.2
3.60	98	0.968	57.1
3.63	140	0.891	70.0
3.77	141	0.889	72.3
3.79	65	0.946	51.4
3.81	68	1.007	50.9
3.83	153	0.982	73.5
4.18	69	0.962	54.2
4.38	101	0.998	56.2
4.50	160	0.956	76.9
4.55	75	0.945	53.7
4.78	72	1.096	52.5

The dependency of the mixture velocity at flashback on three parameters—pressure, temperature, and equivalence ratio—makes trends in the data very difficult to observe. An attempt was made to describe the equivalence ratio at flashback as a function of combustor loading, as suggested by Plee and Mellor [6], but the data were not well correlated. Instead, a regression was performed to define the mixture velocity at flashback as a second-order function of pressure, temperature, and equivalence ratio. Using the mathematical software, MathcadTM, the following function was defined for the mixture velocity at flashback, u_F :

$$u_F = -0.1689 \cdot \phi \cdot T + 0.03188 \cdot P \cdot T + 0.00081 \cdot T^2 + 0.09738 \cdot T + 0.2304 \cdot \phi \cdot P - 1.628 \cdot P^2 + 12.582 \cdot P - 10.444 + 67.769 \cdot \phi - 38.029 \cdot \phi^2 \quad (5.1)$$

where ϕ is equivalence ratio, T is inlet temperature in degrees C, and P is upstream pressure in atm. This relationship is most accurate within the range of conditions tested. Extrapolation to points far outside the tested range is likely to produce significant error, due to the complex nature of the dependencies.

The function defining mixture velocity at flashback can be used to define three-dimensional surfaces that represent the flashback limit at constant equivalence ratios. One such surface is shown in Figure 5.2. The surface shows the mixture velocity at flashback versus inlet temperature and pressure for an equivalence ratio of 0.9. At operating points above the surface, the mixture velocity is sufficient for the flame to stabilize normally on the premixer and allow safe operation. At points below the surface, mixture velocities are too low for stable operation and premixer flashback is expected.

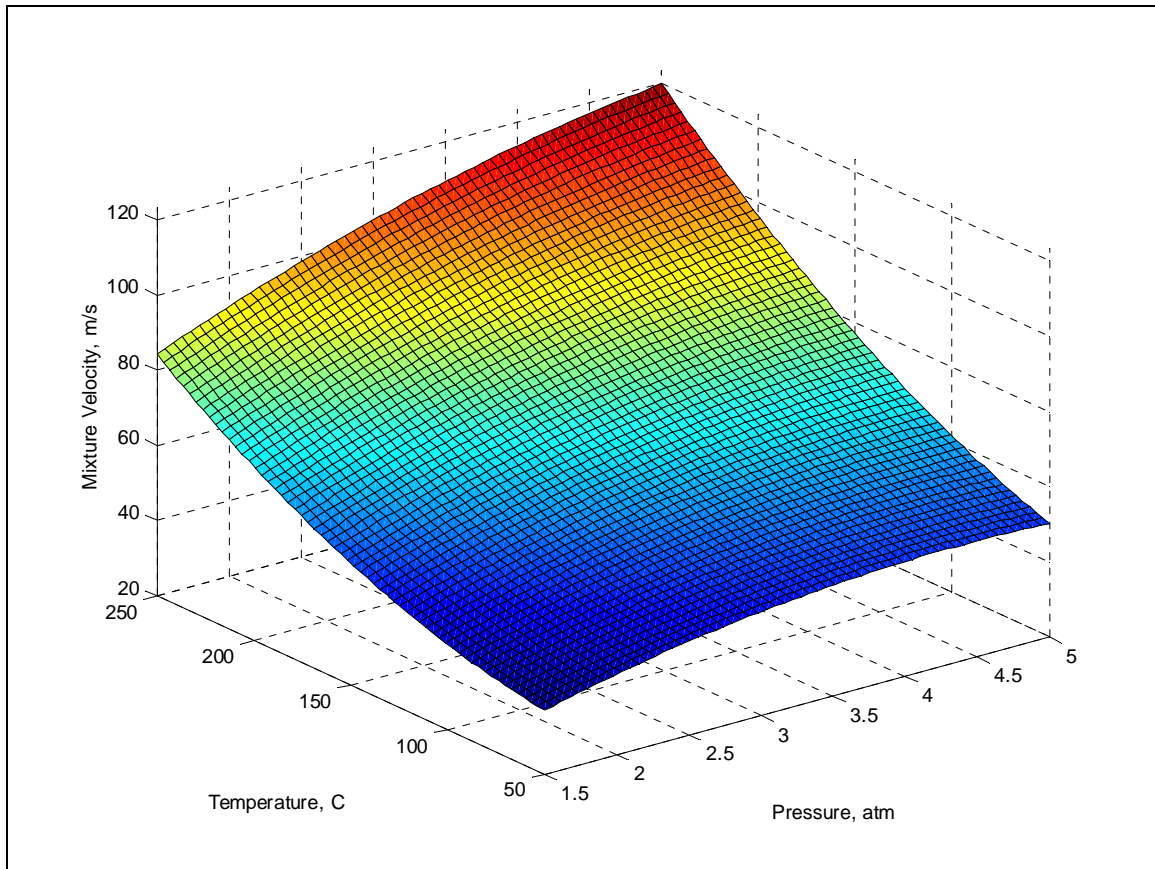


Figure 5.2. Flashback boundary surface for an equivalence ratio of 0.9.

From Figure 5.2, the dependence of the mixture velocity at flashback on temperature and pressure is clear. For a constant equivalence ratio, the flashback mixture velocity shows a nearly linear increase with increasing inlet temperature. This is expected, as increased inlet temperature typically increases burning velocity [2]. The effect of pressure on flashback mixture velocity shows the same trend as the temperature effect, but to a lesser degree. It is somewhat unexpected for the flashback velocity to show an increasing trend with pressure, since burning velocity typically decreases with increasing pressure [2]. However, the tests in the current investigation were performed in a relatively narrow pressure range. Additionally, effects of the premixer geometry on the flow field can affect the tendency toward flashback as pressure changes.

The dependence of flashback mixture velocity on equivalence ratio can be seen in Figure 5.3. The plot shows increasing mixture velocity at flashback as equivalence ratio decreases. This is not the expected trend. However, the equivalence ratio effect appears to be quite small relative to the pressure and temperature effects. An increase in equivalence ratio from 0.6 to 1.0 decreases the mixture velocity at flashback by a maximum of approximately 15 m/s. The differences over the majority of the domain are considerably less. Limitations of the test setup prevented the observation of flashbacks at lower equivalence ratios, which may have improved this aspect of the correlation.

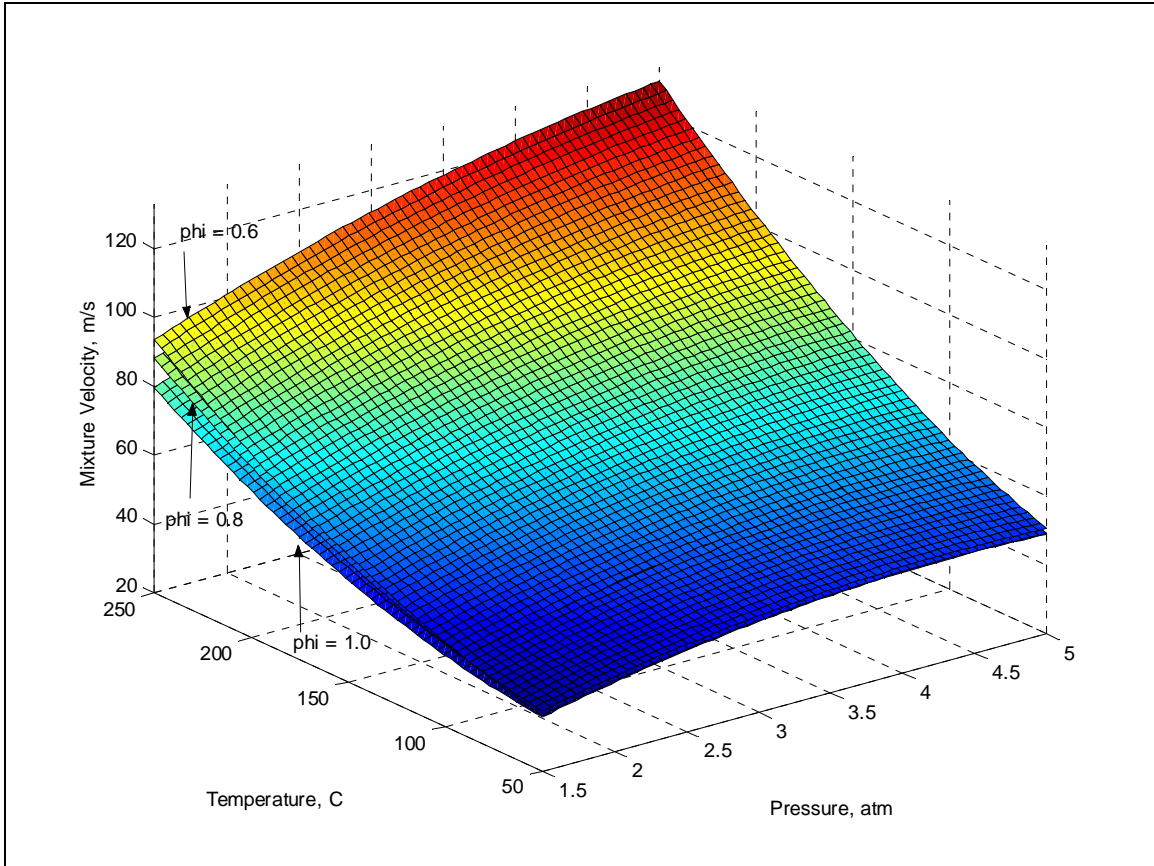


Figure 5.3. Dependence of flashback mixture velocity on temperature and pressure at equivalence ratios of 0.6, 0.8, and 1.0.

Another potential explanation for the locations of the flashback boundary surfaces shown in Figure 5.3 is that the trend of decreasing flashback mixture velocity with increasing equivalence ratio is correct for high equivalence ratios. Figure 5.4 shows the center body of a premixer that suffered a flashback. It is clear from the oxidation that the flame stabilization during a flashback occurs in the wake regions of the fuel jets. At high overall equivalence ratios, it is likely that the equivalence ratios in these regions considerably exceed 1.0. Locally low burning velocities may require a significantly decreased mixture velocity to allow flame propagation into this region. This would not be the expected behavior at lower overall equivalence ratios.

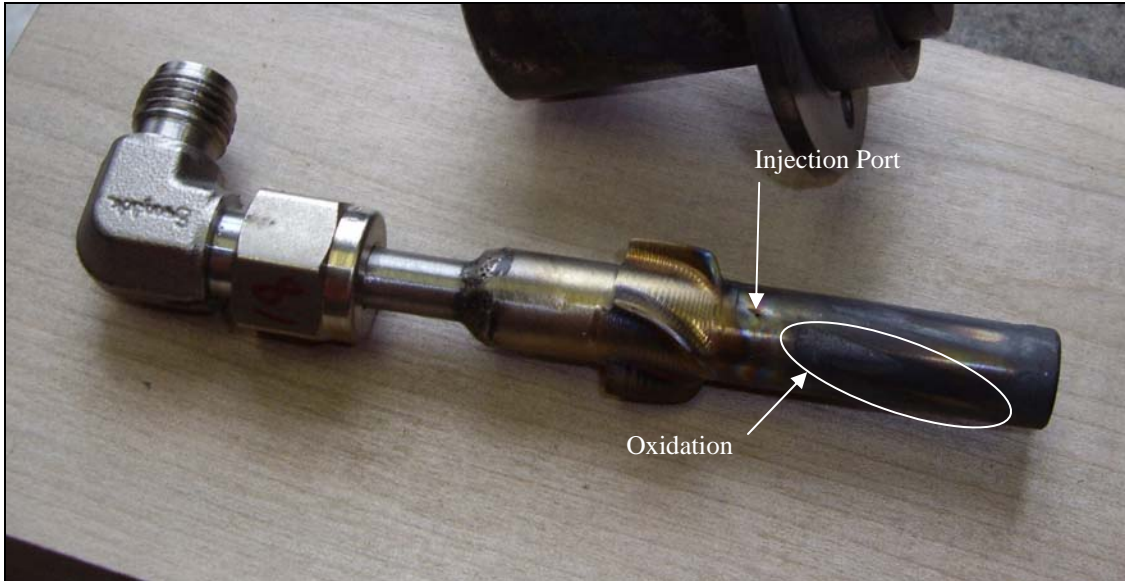


Figure 5.4. Premixer center body after experiencing flashback.

5.2 Discussion of Premixer Test Results

Tests at the CSDL facility showed that premixer flashback was difficult to produce except at conditions that deviated significantly from design operation. Flashbacks were only observed at equivalence ratios above 0.6, pressures greater than 2.6 atm, and inlet temperatures higher than 50 degrees C. While flashbacks are possible at equivalence ratios lower than 0.6, the required mixture velocities are less than 50 m/s, the approximate lower limit on velocity in the test setup. Similarly, greater control of low air flow would be necessary to observe flashback at pressures below 2.6 atm. It was noted that in unheated tests, reversal of the fuel flow into the upstream region of the premixer and subsequent ignition of the flammable mixture in the plenum region occurred instead of flashback.

The test data showed that flashback occurred at higher mixture velocities as inlet temperature was increased. This is an expected effect of the increase in burning velocity associated with the higher temperatures. The pressure effect on the mixture velocity at flashback showed the same trend as the temperature effect, but was less significant.

While burning velocity has generally been observed to decrease with increasing pressure, the effect is small. The relatively narrow pressure range of the tests suggests that flow field features, rather than burning velocity variations contribute to the trends observed. The equivalence ratio effect was unexpected, showing increasing tendency toward flashback at lower equivalence ratios. Given the high overall equivalence ratios tested, however, it is possible that local equivalence ratios in the premixer annulus considerably exceeded stoichiometric. This would decrease the burning velocity in the wake regions of the fuel jets and lower the required mixture velocity for flashback at higher equivalence ratios.

5.3 Results of the Engine Tests

The tests performed using the modified Pratt and Whitney Canada PT6A-20 examined the interaction between the engine and premixers. Tests using pure hydrogen allowed successful operation of the engine and premixers up to 150 hp. The operation of the premixers in the engine was limited by flashbacks, which consistently occurred at the 150 hp level. Flashbacks never occurred between light-off and idle and rarely at power levels less than 150 hp. During all tests where flashbacks occurred, the flashback was successfully disgorged using the procedure described in Section 4.4. Specifically, fuel was removed from the affected premixers, the power level was returned to idle, and the affected premixers were re-lit. This procedure consistently returned engine and premixer operation to normal without damage.

One goal of the engine tests was to compare the performance of the unmodified engine (burning Jet-A) to the engine after modification with the premixers. Figure 5.5 shows compressor outlet pressure versus shaft power for the engine operating on Jet-A (unmodified) and hydrogen (modified). The plot shows a slight elevation in the compressor outlet pressure of the modified engine over the majority of the operating range. This is consistent with an increase in the combustor pressure drop. In fact, static taps measured a relative pressure loss of 5.0 percent across the liner and premixers, a notable increase from the specified 2.0 percent for the unmodified engine. The

discrepancy in the data sets at very low power levels is likely the result of increased inter-stage compressor bleed flow resulting from the higher combustor pressure loss.

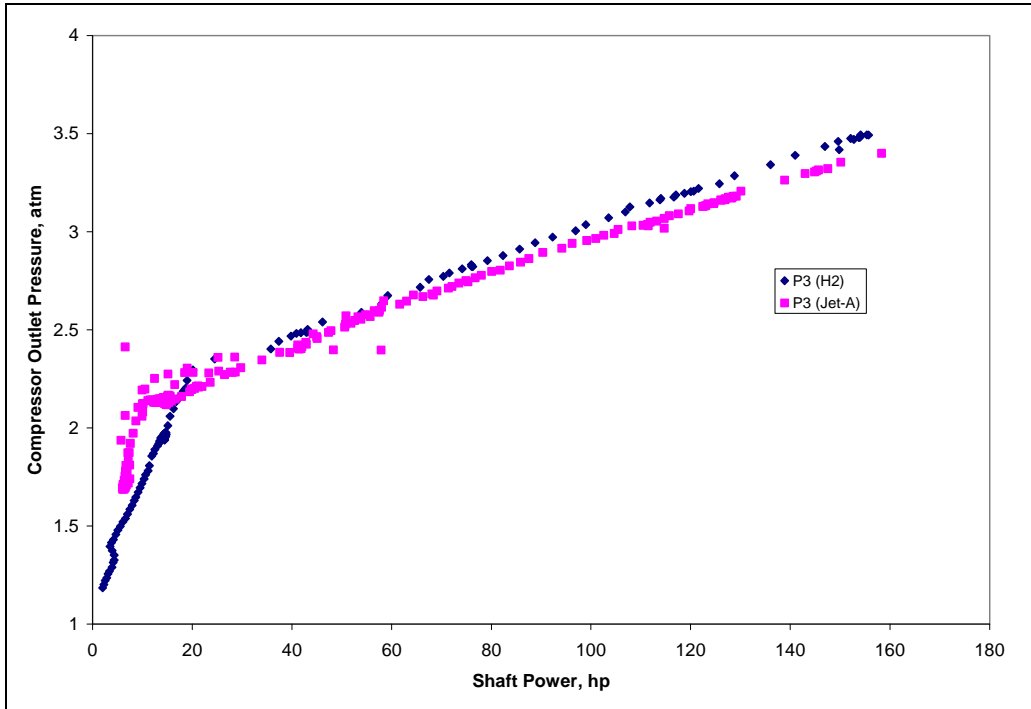


Figure 5.5. Plot of compressor outlet pressure versus shaft power for the PT6A-20 operating on Jet-A and hydrogen.

Figure 5.6 is a plot of compressor outlet temperature versus shaft power for the unmodified and modified engine. Throughout most of the operating range, the compressor outlet temperature during the test of the unmodified engine was about 20 degrees C higher than in the test of the modified engine. This is not considered to be a result of the modifications to the combustor, rather, it is a result of operating procedure. In the test of the unmodified engine, significant time was spent in the power range between idle and 60 hp. During this time, heat transfer from the compressor air increased the temperature of the compressor components and gas generator case (called heat soak), resulting in an elevation of the compressor outlet temperature. The compressor outlet temperature of the unmodified engine remained elevated relative to the temperature of the modified engine throughout the eventual acceleration to 150 hp (indicated by a callout). No conclusions about engine performance can be drawn from this comparison, since both data sets represent transients. It should be noted, however, that the other operational data

discussed here can be reasonably compared. Engine tests have shown that the time scales associated with the other parameters are relatively short and the data can be considered quasi-steady.

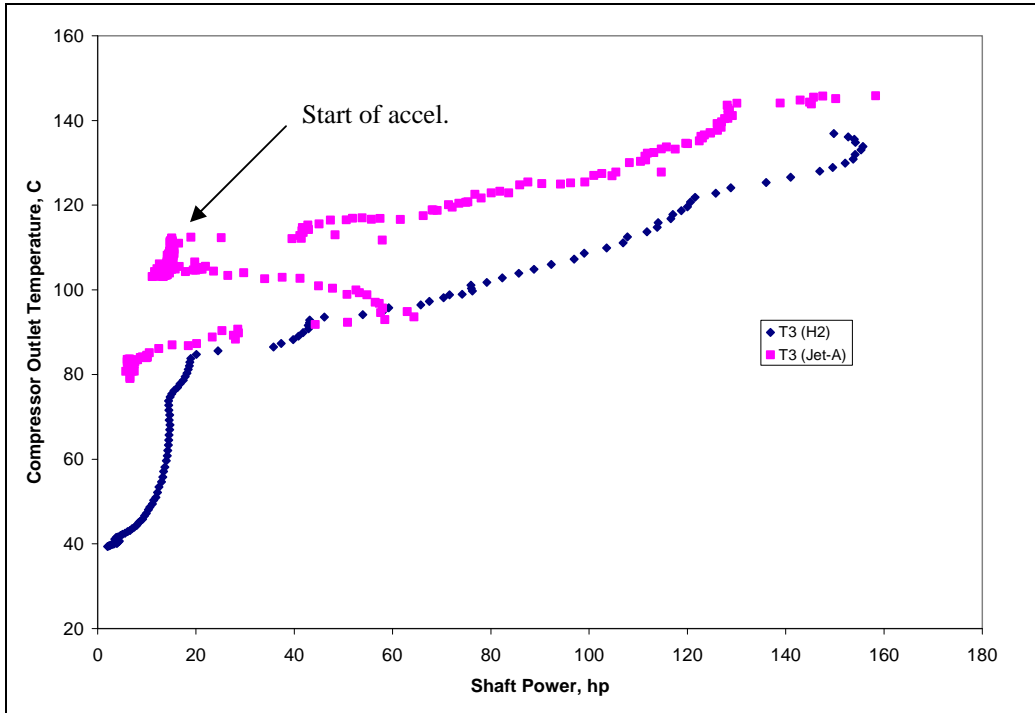


Figure 5.6. Plot of compressor outlet temperature versus shaft power for the modified and unmodified engine.

Figure 5.7 is a plot of fuel flow versus power for the unmodified and modified engine. The fuel flow for the unmodified engine has been converted to an equivalent hydrogen flow based on lower heating value in order to provide a more direct comparison. The unmodified and modified engine data show similar trends. However, the energy equivalent fuel flow required by the unmodified engine is consistently higher than that required by the modified engine. This is contrary to the expected behavior, since the increased combustor pressure loss in the modified engine should result in lower thermal efficiency and higher fuel requirements for a given power level. A difference in combustion efficiency between the two fuels is unlikely to account for the difference. Though the combustion efficiency of the unmodified engine is likely to be decreased at off-design conditions, the effect on fuel flow should be relatively small. The simplest

and most likely explanation is a problem with the hydrogen metering equipment which resulted in inaccurate measurements.

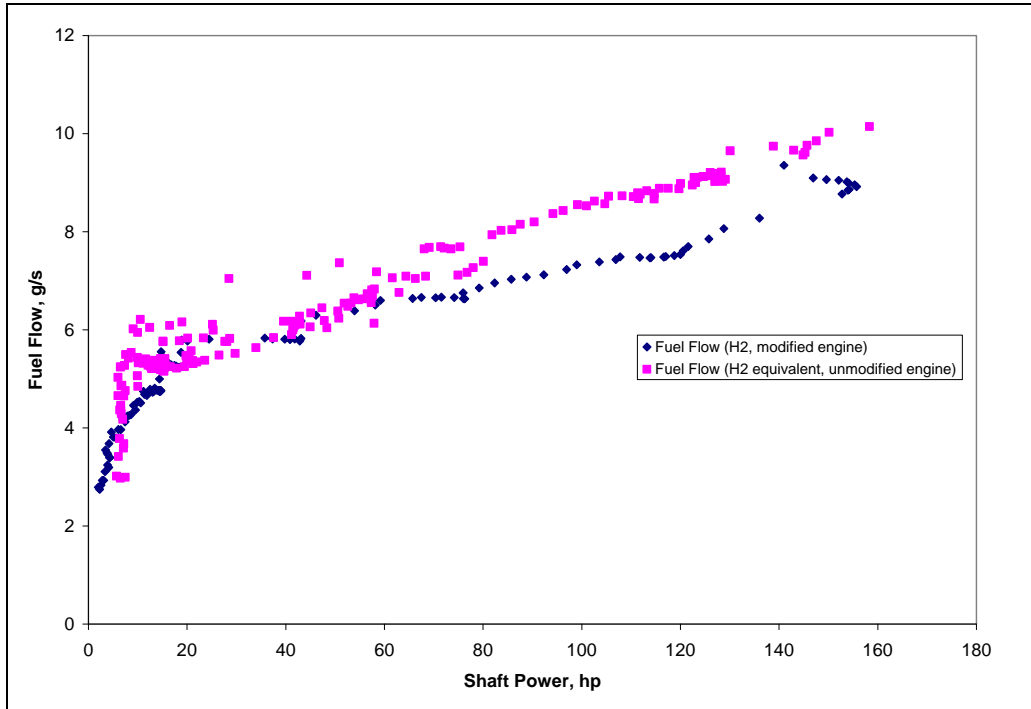


Figure 5.7. Plot of fuel flow versus shaft power for the modified and unmodified engine.

Figure 5.8 is a plot of gas generator speed versus power for the modified and unmodified engine. The plot shows that the modified engine consistently operated at a slightly higher gas generator speed than the unmodified engine at a given power output. The disparity is approximately three percent of N_g at most power levels and is an expected result of the higher combustor pressure loss in the modified engine. The increased pressure loss of the modified combustor decreases the mass flow of air available to the power turbine at a given gas generator speed. As a result, higher gas generator speeds are required to attain given power levels.

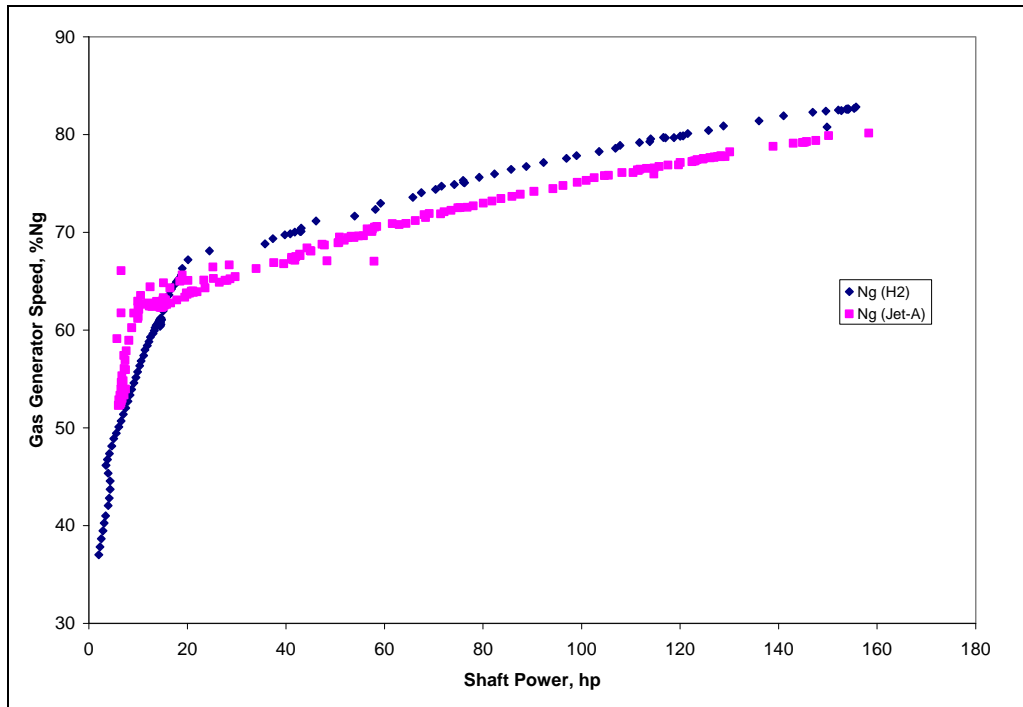


Figure 5.8. Plot of gas generator speed versus shaft power for the modified and unmodified engine.

Figure 5.9 shows the steady-state NO_x production versus shaft power for the engine before and after combustor modification. The data shows that the use of lean premixed hydrogen combustion contributed to a reduction in NO_x emissions to as little as 15 percent of the level produced by Jet-A. In addition to the contribution of lean premixed combustion, fast dilution of the combustion products may also have inhibited NO_x production in the modified engine. The combustor liner used with the lean premixed system was shortened (2.7 inches versus 8.0 for the unmodified liner) and incorporated a large amount of dilution immediately downstream of the premixers. This was possible due to the rapid burning of the hydrogen and the associated short flame lengths.

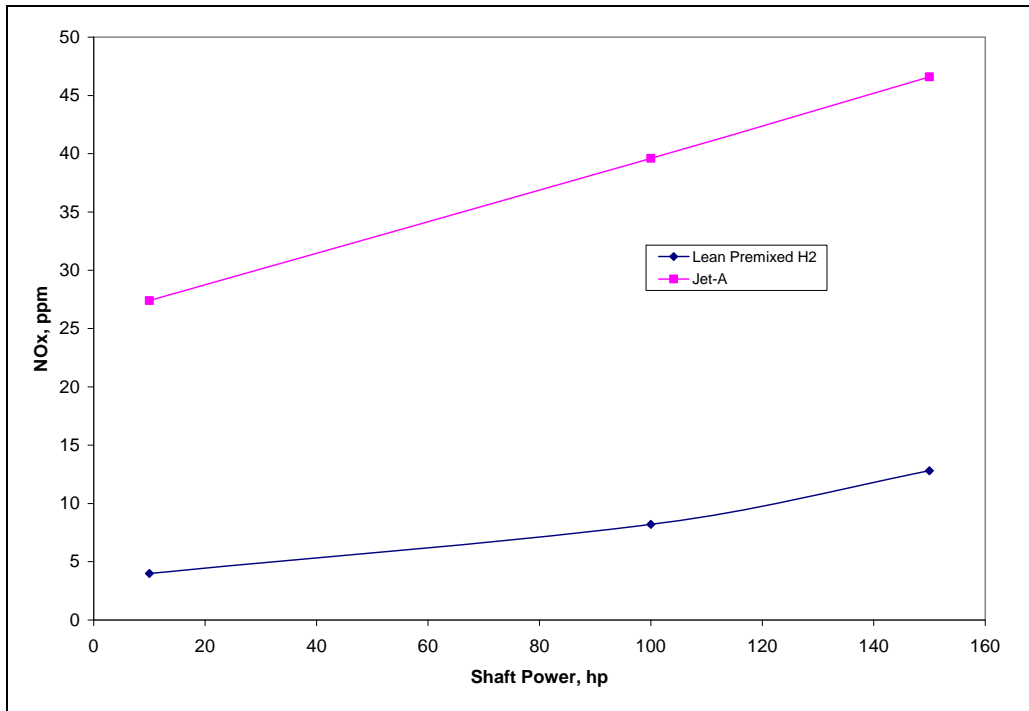


Figure 5.9. Plot of NO_x production versus shaft power for the engine before and after combustor modification.

5.4 Discussion of the Engine Test Results

The engine tests showed that successful operation of the modified engine using pure hydrogen was possible at power levels up to 150 hp. Premixer flashback at this power level consistently limited engine operation. However, operation was always stable between light-off and idle and generally stable at low power levels. The engine data showed an increase in the compressor outlet pressure over the engine's operating range as a result of the engine modifications. This suggests an increase in throttling downstream of the compressor caused by an increase in combustor pressure loss (measured by static taps as 5.0 percent of upstream). An accompanying decrease in air flow is supported by the increase in gas generator speed also seen over the engine's operating range. NO_x levels were significantly reduced in the modified engine, but were still higher than the ideal levels of less than 1 ppm suggested in the literature [4]. This, along with the occurrence of flashback indicates that operating equivalence ratios were higher than design.

5.5 Computer Model Results: Unmodified Engine Performance

The computer engine model was used as a tool to predict and evaluate the performance of the modified engine and premixers. Before the computer model could be used for this purpose, it was necessary to validate the model with known engine performance data. A large amount of data was collected during tests of the unmodified engine and served as an excellent tool to validate the model's predictions of off-design performance.

Figure 5.10 is a plot showing the actual and predicted compressor outlet pressure versus shaft power for the unmodified engine operating on Jet-A. It is clear that the model makes a very accurate prediction of compressor outlet pressure over the engine's entire operating range. The model prediction deviates from the actual performance only at very low power levels. This discrepancy is not unexpected, since far off-design performance is very difficult to predict. At idle, engine operation is barely self-sustaining and is strongly dependent on the characteristics of the turbomachinery and the bleed schedule.

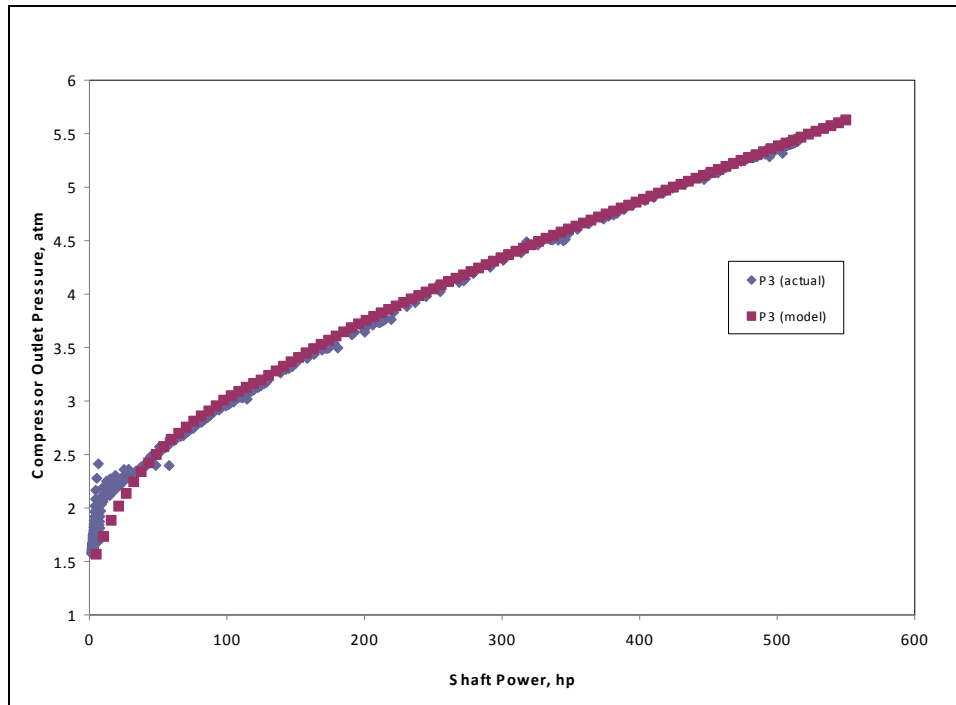


Figure 5.10. Plot of actual and predicted compressor outlet pressure versus shaft power for the unmodified engine.

Actual and predicted values of fuel flow versus shaft power for the unmodified engine are plotted in Figure 5.11. The data show strong agreement throughout the engine's operating range, with small variations at low and moderate power levels. The low power level discrepancy is, again, likely a result of the difficulty in predicting the very low-speed performance of the turbomachinery. The slightly lower fuel flows predicted by the model at moderate power levels indicate that the component maps used by the model tend to slightly over-predict off-design efficiency.

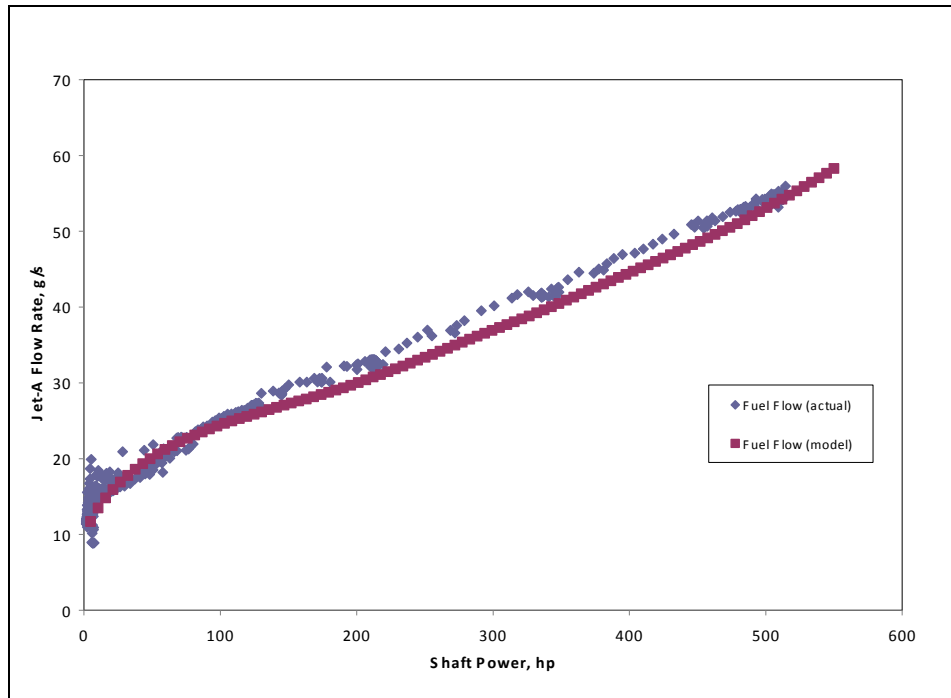


Figure 5.11. Plot of actual and predicted Jet-A flow versus shaft power for the unmodified engine.

Figure 5.12 is a plot of predicted and actual compressor outlet temperature versus shaft power. Initial inspection of the data suggests significant discrepancies between the model predictions and actual engine performance. The discrepancies, however, are the result of the fact that much of the recorded engine data occurred during transient operation. The steady values of compressor outlet temperature (indicated with callouts) actually agree very closely with the model's steady-state predictions. As previously stated, compressor outlet temperature displayed a long time scale relative to the other performance parameters, requiring approximately four minutes of operation to reach steady state. While this temperature data must be considered transient, data associated with the other parameters may be considered quasi-steady.

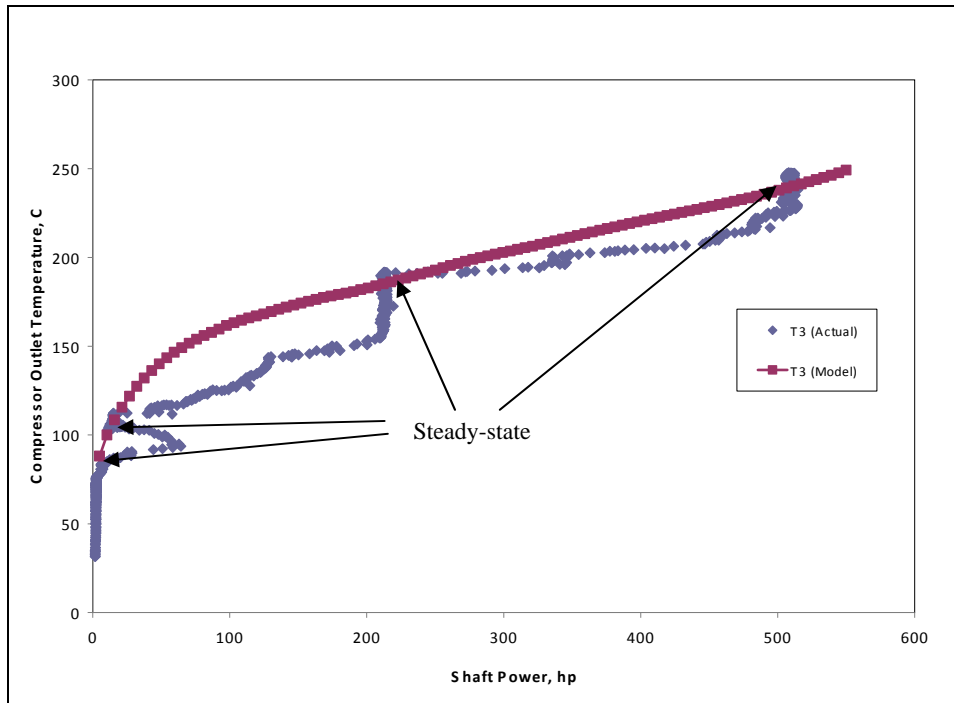


Figure 5.12. Plot of actual and predicted compressor outlet temperature versus shaft power for the unmodified engine.

The only significant disagreement between the model predictions and the recorded engine data is seen in Figure 5.13, which is a plot of gas generator speed versus shaft power. The plot shows a noticeable offset in gas generator speed over the entire operating range of the engine. This is explained by the fact that the gas generator speed at a given power level is heavily dependent on the aeromechanical characteristics of the turbomachinery. The discrepancy results from differences between the model's component maps and the characteristics of the actual compressor and turbines. To provide the best accuracy, the analyses in this investigation that are made using the model are based on shaft power, rather than gas generator speed.

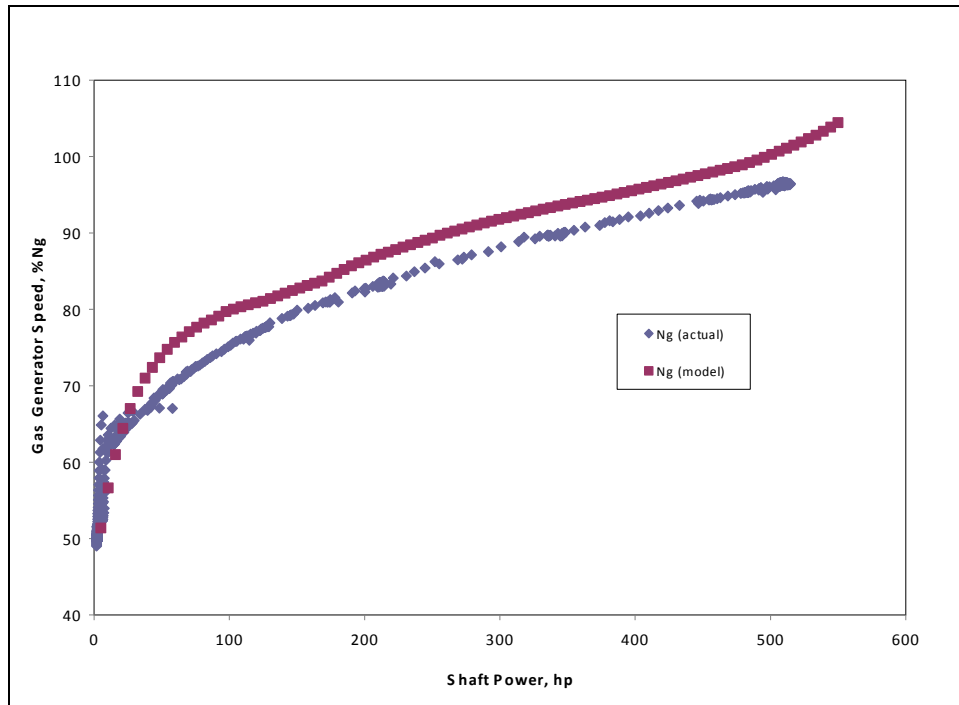


Figure 5.13. Plot of actual and predicted gas generator speed versus shaft power for the unmodified engine.

A final important model prediction for the unmodified engine is the air flow rate versus power, shown in Figure 5.14. The plot shows only predicted data, since no accurate measurement of the off-design air flow through the test engine was possible. The lack of an air flow measurement is significant, since air flow is an important part of the premixer performance analysis. However, the good agreement of the other engine performance predictions with the test data suggests that a reasonable level of confidence in the air flow prediction is warranted. It should be noted that the inter-stage bleed schedule was also unknown and was specified as 20 percent of the inlet air flow at idle, decreasing linearly to zero at 150 hp. This schedule was an estimate based on maintaining consistent stall margin along the operating line of the simulated engine.

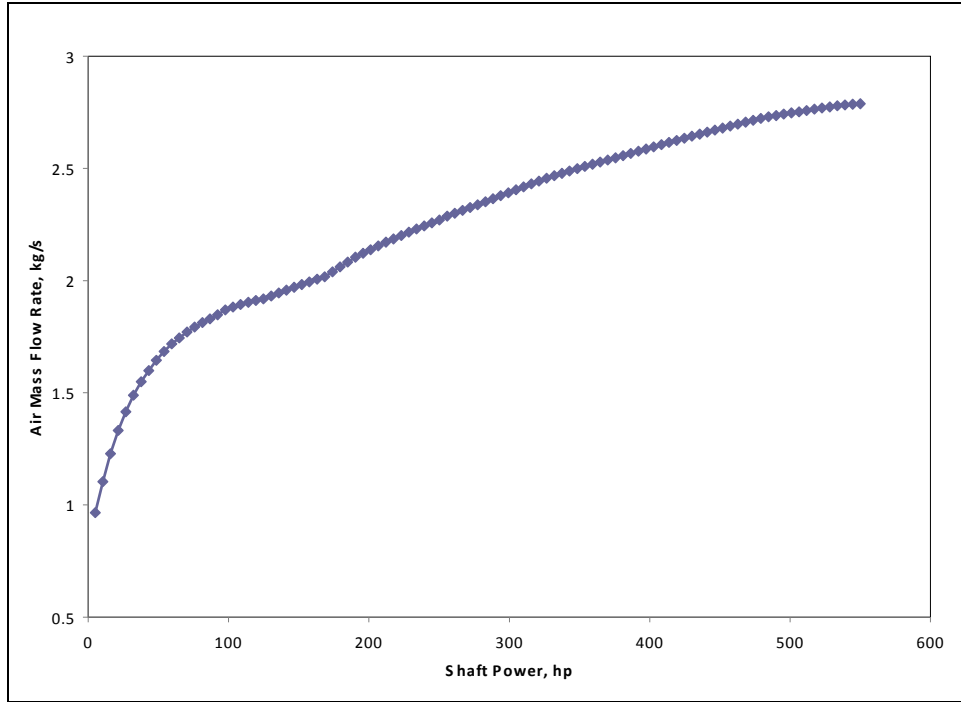


Figure 5.14. Plot of predicted air mass flow versus shaft power for the unmodified engine.

5.6 Computer Model Results: Modified Engine Performance

After validation based on data from the unmodified engine, the computer model was used to predict the performance of the modified engine operating on hydrogen. To model the modified engine, the design point inputs for the engine were left unchanged. The off-design combustor relative pressure loss was increased from 2.0 percent—the level specified for the unmodified engine—to 5.0 percent, which corresponds to the level measured in the modified engine. The fuel was changed from Jet-A to hydrogen. While the operability of the test engine was limited to 150 hp, the model predictions cover the entire operating range of the engine (up to 550 hp). This is possible since the premixer flashback stability is not a part of the engine model.

Figure 5.15 shows the actual and predicted values for compressor outlet pressure versus shaft power in the modified engine. The agreement between the actual and

predicted data is very good at power levels above 50 hp. Below 50 hp, the pressure roll-off predicted by the model is significantly more gradual than what is seen in the data. This appears to be a response of the inter-stage compressor bleed system to the increase in combustor pressure loss. Since the system is not well-known, its behavior could not be fully incorporated into the model. Fortunately, the bleed flow is not significant at power levels above about 100 hp. This suggests that the model predictions would continue to be accurate at higher power levels if engine operation were possible in that range.

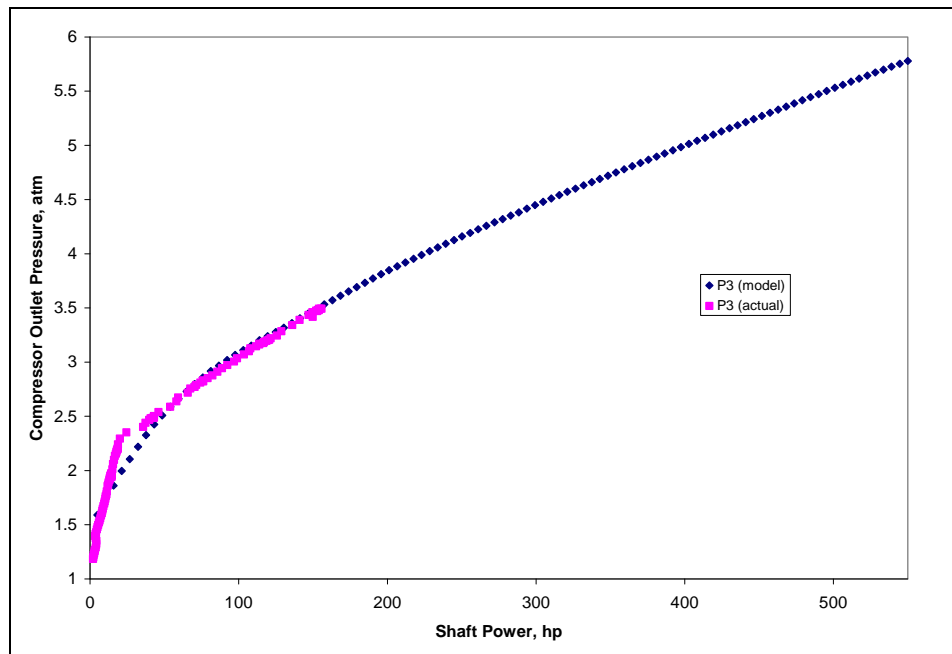


Figure 5.15. Plot of actual and predicted compressor outlet pressure versus shaft power for the modified engine.

A plot of predicted and actual compressor outlet temperature versus power for the modified engine is shown in Figure 5.16. As for the previous comparisons of actual and predicted compressor outlet temperature, the transient nature of the engine run data makes a direct comparison with the model difficult. Given the model's accurate predictions of the steady-state compressor outlet temperature of the unmodified engine, however, it is reasonable to accept the predictions for the modified engine as accurate. Realistically, the combustor modifications are likely to affect the compressor discharge temperature less than the pressure (since temperature effects are small relative to pressure

effects in the compression process). Indeed, the model predicts steady-state compressor outlet temperatures very similar to those of the unmodified engine.

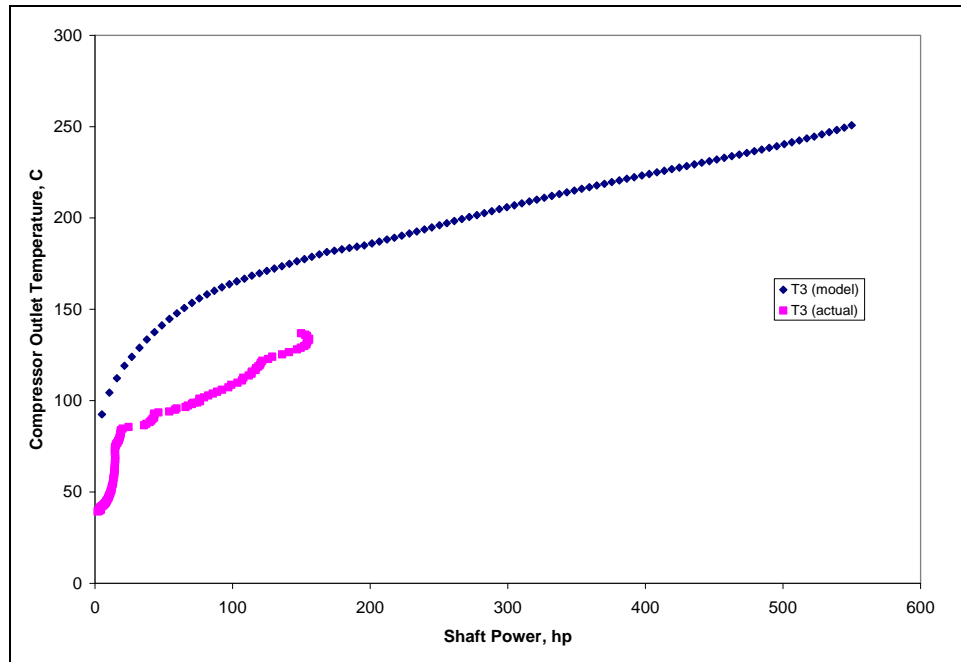


Figure 5.16. Plot of actual and predicted compressor outlet temperature versus shaft power for the modified engine.

Figure 5.17 shows the actual and predicted values of fuel flow versus shaft power for the modified engine. The data agree below power levels of about 20 hp, but deviate significantly at higher power levels. It is not likely that the model over-predicts the fuel flow rate, since the predicted flow rates (in terms of energy equivalence) are not significantly different from those for the unmodified engine. Instead, as previously discussed, the discrepancy likely reflects a problem with the hydrogen flow rate measurement.

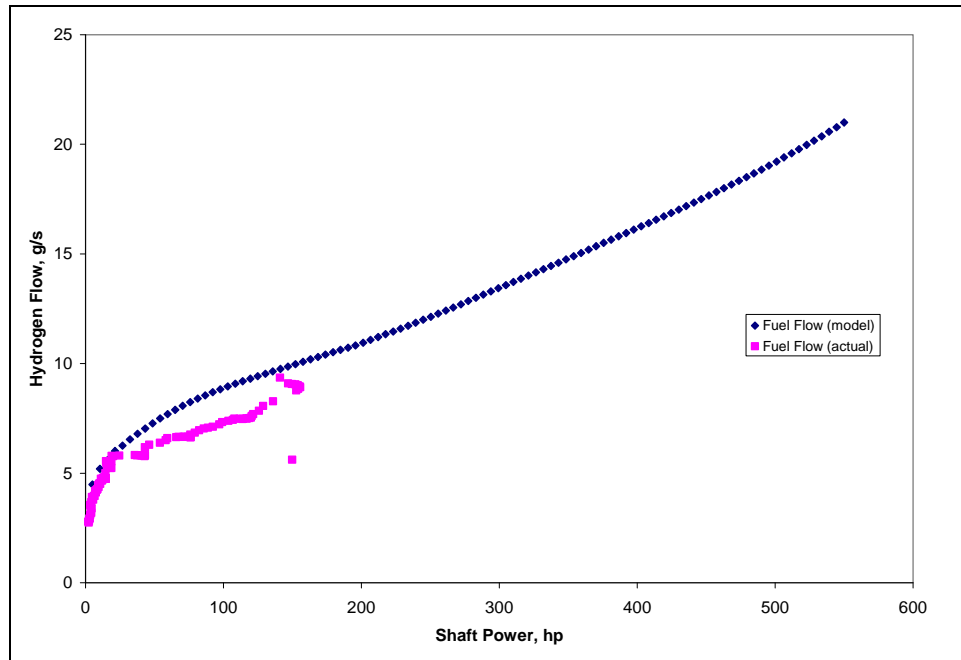


Figure 5.17. Plot of actual and predicted hydrogen flow versus shaft power for the modified engine.

While no air flow data were recorded during the engine tests, the effect of the engine modifications on air flow is important to the investigation. Air flow affects the performance of the premixers, as well as the post-combustor temperatures in the engine. Figure 5.18 shows the model prediction of the air flow versus power for the modified and unmodified engine. The predicted results are as expected, with the increase in combustor pressure loss leading to a small decrease in the air flow rate at all power levels. The decrease in air flow is somewhat larger at low power levels, both on an absolute basis and as a percentage of the air flow in the unmodified engine. This is expected, since increased throttling tends to more strongly affect compressor air flow at low speeds due to the characteristics of the turbomachinery [13].

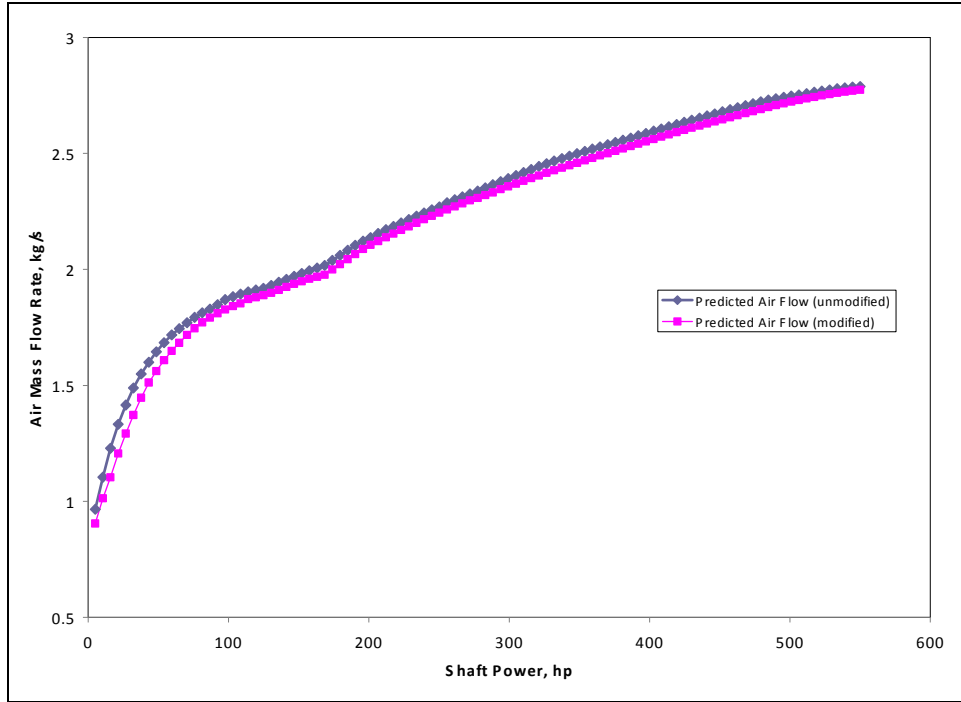


Figure 5.18. Plot of the predicted air flow versus power for the unmodified and modified engine.

5.7 Computer Model Results: Premixer Performance

Knowledge of the premixer flashback limits, as well as an accurate model of engine performance provides the basis for an analysis of the operability limit of the premixers in the modified engine. As a first step, it is useful to examine the operating conditions the premixer would experience in the engine given a design premixer equivalence ratio of 0.4 at full power conditions. A premixer equivalence ratio of 0.4 at full power (where the overall equivalence ratio is 0.26) requires that 64.7 percent of the total combustor air pass through the premixers and the remaining 35.3 percent pass through the combustor liner. Tests have shown that the flow split remains approximately constant over the operating range of the engine.

Figure 5.19 shows the variation in equivalence ratio and axial mixture velocity at the premixer exit versus power. The plot is based on a design full power premixer equivalence ratio of 0.4 and the operating parameters (fuel flow, total air flow,

compressor outlet temperature, and compressor outlet pressure) predicted by the computer model of the modified engine. The plot shows very high mixture velocities and very low equivalence ratios across the entire range of operation of the engine. These conditions are far from any of the conditions where flashbacks were observed in the laboratory experiments. This suggests that the flow split between the premixers and liner in the modified engine is not near the design value of 64.7 percent to 35.3 percent. This idea is further supported by the fact that the very high mixture velocities shown in the plot would be nearly impossible to attain in the engine. The relative pressure loss associated with the full-power mixture velocity is at least 14.7 percent (based on isentropic flow). This level of pressure loss would likely cause compressor stall and prohibitively high internal temperatures.

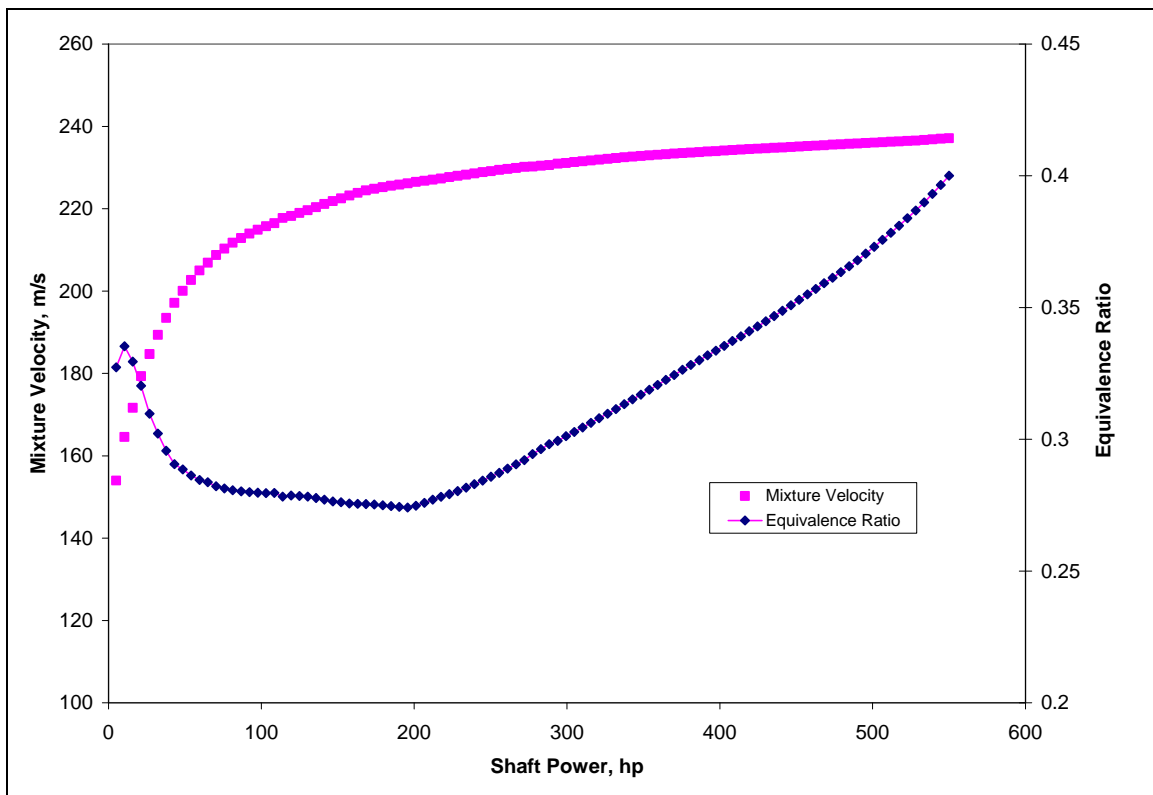


Figure 5.19. Plot of equivalence ratio and mixture velocity at the premixer exit versus power for a full-power premixer equivalence ratio of 0.4.

The consistent flashbacks encountered at 150 hp during the engine tests suggest, according to the laboratory stability tests, that the operating equivalence ratios in the

engine are much higher than design and the mixture velocities are much lower. It is possible to use data from the laboratory tests, engine tests, and engine model to deduce the true operating conditions of the premixers in the engine. As previously noted, from the combustion lab tests it is known that the mixture velocity at the flashback limit, u_F , can be described as follows:

$$u_F = f(P, T, \phi) \quad (4.1)$$

where the specific dependence of u_F on pressure, P , temperature, T , and equivalence ratio, ϕ , is given by Equation 5.1. It can also be shown that in general, the mixture velocity at the premixer exit, u_m , is given by:

$$u_m = \frac{\dot{m}_f R_m T}{P \cdot A} \left(1 + \frac{1}{\phi (F/A)_{stoich}} \right) \quad (5.2)$$

where \dot{m}_f is the mass flow rate of hydrogen through each premixer, R_m is the ideal gas constant of the mixture, A is the exit area of one premixer, and $(F/A)_{stoich}$ is the stoichiometric fuel-to-air ratio for hydrogen, equal to 0.0292 kg H₂ per kg air. For an operating point at the flashback limit, u_m equals u_F , and Equations 5.1 and 5.2 can be solved simultaneously to determine the mixture velocity and equivalence ratio. At the 150 hp condition, doing so yields a premixer equivalence ratio of 0.88 and a mixture velocity of 84.8 m/s.

The equivalence ratio of 0.88 and mixture velocity of 84.8 m/s at the 150 hp condition indicate that the premixers in the modified engine receive only 20.2 percent of the total combustor air flow, while the liner receives 79.8 percent. Figure 5.20 shows the variation in mixture velocity and equivalence ratio at the exit of the premixer over the operating range of the engine based on this air flow split. Based on the model predictions, the premixer equivalence ratio is much higher than the design value over the entire operating range, varying between approximately 0.85 and 1.3. The mixture velocities are much lower than design, ranging from approximately 60 m/s to 95 m/s. These mixture velocities are less than half the design velocities. It should be noted that the increase in mixture velocity above about 200 hp is due, in large part, to the increasing equivalence ratio, which decreases the molecular weight of the mixture. The effect is

more significant, relative to the idle mixture velocity, than in the lower equivalence ratio (design) case.

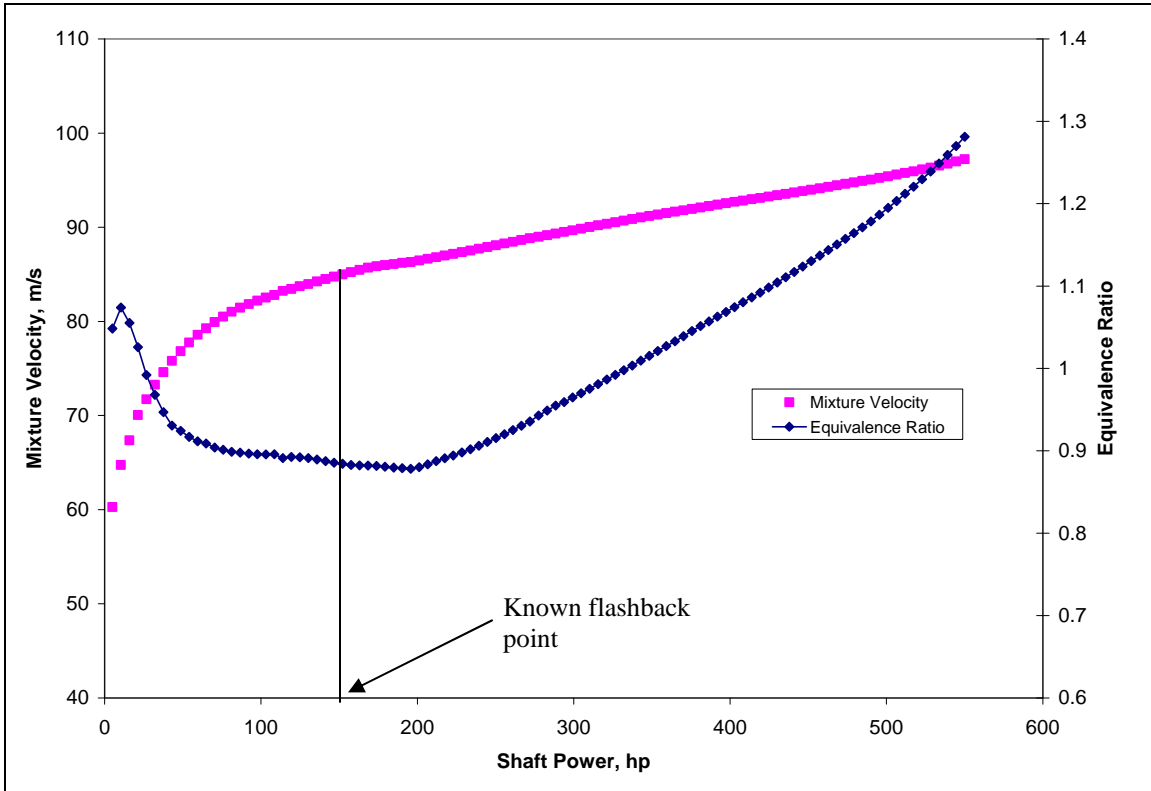


Figure 5.20. Plot of equivalence ratio and mixture velocity at the premixer exit versus shaft power for a premixer flow split of 20 percent.

Analysis of the variation of equivalence ratio and mixture velocity over the engine's operating range raises the issue of operability at power levels above 150 hp. Since flashback limited the operation of the modified engine to lower power levels, it was never directly determined whether a region of stable operation existed at higher power levels. Though exploration of this prospect was not possible in the engine tests, it can be predicted based on the current analysis.

Figure 5.21 is a plot of the premixer exit mixture velocity and the flashback mixture velocity over the engine's operating range. The plot shows that after the crossing of the two curves (the point where flashback is first predicted to occur), the premixer exit velocity is always lower than the flashback velocity. This means that stable operation at

higher power levels is not possible. If the curves did cross again at a higher power level, it is still unlikely stable operation could be achieved there. When a flashback occurs, a Rayleigh-type flow is created in the premixer annulus. This increases the pressure loss of the premixer [15] and increases the percentage air flow through the combustor liner. As a result, flashbacks cannot be disorged by acceleration of the engine.

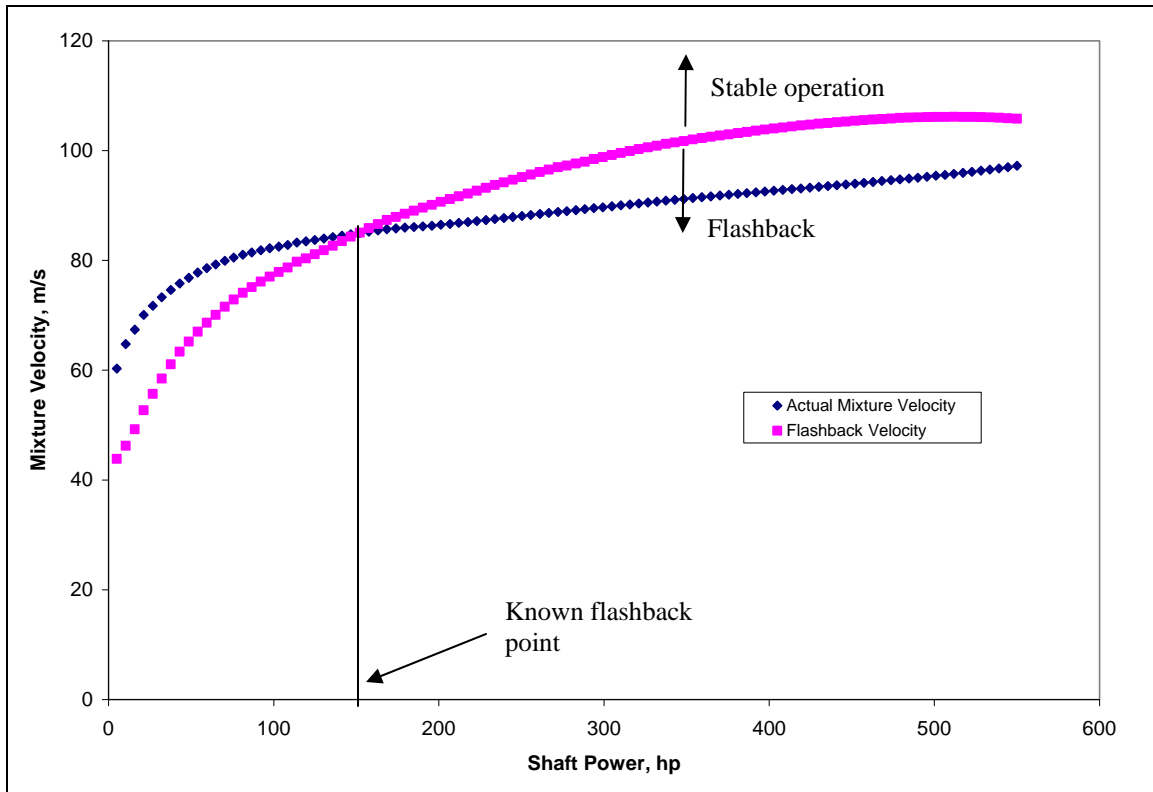


Figure 5.21. Plot of actual mixture velocity and flashback mixture velocity versus shaft power for a premixer flow split of 20 percent.

5.8 Discussion of Computer Model Results

The computer engine model showed a high level of accuracy predicting the performance of the unmodified engine. Similarly, the model showed good agreement with the data gathered from the modified engine. The ability of the model to predict engine operation supports the validity of the final analysis, which examines the operation of the premixers in the engine. The computer model and flashback data combine to show

that the internal premixer equivalence ratios produced in the modified engine are far off-design. The equivalence ratio at the 150 hp level, where flashbacks consistently occurred, is calculated as 0.88, with only 20 percent of the total engine air going to the premixers. This is in stark contrast to the design air flow split, in which over 60 percent of the total engine air was intended to pass through the premixers. This suggests a poorly-matched combustor liner and premixer internal flow path design. The combustor liner produces too little premixer air flow and the premixer design velocities are prohibitively high to achieve the correct flow split. The model indicates that stable operation of the premixers in this engine is not possible at any power level over 150 hp with the current design.

Chapter 6: Conclusions and Recommendations

This chapter reviews the work conducted in the current investigation. The first section is a discussion of the results of the investigation, their validity, and their significance to the continued development of a lean premixed combustion system for a turbine engine. The second section presents recommendations based on the investigation and potential future work that will further the understanding of the topic.

6.1 Conclusions

An investigation has been conducted to examine the operation of a hydrogen-air premixer designed for use in a lean-premixed combustion system for a modified Pratt and Whitney Canada PT6A-20 turboprop engine. Experiments were carried out at the Combustion Systems Dynamics Laboratory to determine the flashback limits of the premixer at conditions related to the operating line of the engine. Then, tests of the premixer in the modified engine were conducted to determine the operability of the engine and premixer. Finally, a computer engine model was created to aid in the analysis of the premixer and engine performance.

The tests carried out at the CSDL facility showed that the premixer has strong flashback stability. In fact, flashbacks were difficult to produce in the test premixer, requiring significant departures from the design operating conditions. Operation was always stable at design conditions, and flashbacks were rarely observed at equivalence ratios less than 0.7 or mixture velocities above 75 m/s. Analysis of the test results showed that the tendency toward flashback increased with increasing inlet temperature as well as with increasing pressure. The analysis also suggested that lower equivalence ratios produced flashbacks at higher mixture velocities. This appears to be a result of the mechanism of flame stabilization in the premixers and is not expected to be valid at lower equivalence ratios. Though limitations of the test setup prevented doing so, tests at lower equivalence ratios and lower mixture velocities may improve the understanding of the effect of equivalence ratio on flashback stability.

Despite expectations based on the premixer laboratory tests, flashback presented a significant barrier to operability of the premixers in the engine. Operating from light-off to idle consistently produced favorable results, with no flashbacks observed in any tests. However, operation at increased power levels was problematic. Flashbacks consistently occurred at the 150 hp level and occasionally before. While operating procedures successfully prevented damage to the engine or premixers as a result of flashbacks, power levels above 150 hp were unattainable in continuous operation. This suggests that the operation of the premixers installed in the modified engine was far off-design. This was shown to be a result of the combined combustor liner design and the premixer internal flow capability, which resulted in too little air flow through the premixers. Despite this, NO_x production was significantly decreased in the modified engine. NO_x production was as little as 15 percent of the NO_x production of the unmodified engine and has the potential to be further reduced by the design operation of the premixers.

The computer model was a very useful tool in the analysis of the modified engine and premixers. The model was validated using data from the unmodified engine and showed the ability to very accurately model its performance. Its predictions of the modified engine's performance also appeared accurate. In conjunction with the data from the premixer stability tests, the model was used to determine that the flashbacks in the engine tests were occurring at an equivalence ratio of 0.88 and a premixer flow split of only 20 percent. This indicates that the premixers passed only about one third of the design air flow. The analysis predicted that mixture velocities above the 150 hp level would remain below the mixture velocity at the flashback limit over the rest of the engine's operating range, and that higher power operation of the engine would result in flashback. This, in fact, was found to be the case..

6.2 Recommendations and Future Work

The investigation showed that the premixer design has strong resistance to flashback. However, operation in the engine was sufficiently off-design to make flashback a barrier to operability. An increase in mixture velocity and a corresponding

decrease in equivalence ratio would likely produce greatly improved premixer stability in engine operation. The simplest way to accomplish this is to decrease the air flow through the combustor liner by decreasing the area of the dilution air holes. The disadvantage of this solution is that it would result in increased combustor pressure loss for a given premixer design. Evidence suggests that increased pressure loss can lead to unacceptable turbine inlet and inter-turbine temperatures in the engine.

Another option that could improve the performance of the premixers in the modified engine is an increase in premixer area, rather than a decrease in combustor liner area. Increasing the premixer area would increase air flow, but not mixture velocity. Laboratory tests showed, however, that the premixer produced a stable flame even at low mixture velocities, provided the equivalence ratio was sufficiently low (near the design value of 0.4). An increase in premixer area would require the use of a similar number of premixers to that used in the current investigation, each with an increased annular area. While an increased number of premixers of the current design would also increase premixer area, the number required to achieve a significant decrease in velocity would be prohibitively large (over 40 for a mixture velocity of 80 m/s).

An additional recommendation is the completion of low equivalence ratio flashback tests. Tests of flashback stability at equivalence ratios between 0.4 and 0.7 would increase the understanding of the trends in mixture velocity at the flashback limit versus equivalence ratio. Since the equivalence ratio at the premixer exit varies considerably over the engine's operating range, this information would be useful in defining the safe operating range of a modified design. Finally, tests that examine the specific mechanism of flashback in the premixer of the current design would be helpful as a predictor of flashback limits in future designs. Since flame stabilization in the wakes of the fuel jets appears to be the mechanism producing flashback in the current design, work should be performed to characterize flame stabilization downstream of jets in a cross-flow, particularly in a channel.

References:

- [1] Ehsani, M. et. al., *Modern Electric, Hybrid Electric, and Fuel Cell Vehicles*, CRC Press: Boca Raton, 2005.
- [2] Turns, S., *An Introduction to Combustion: Concepts and Applications*, 2nd ed., McGraw-Hill: Singapore, 2000.
- [3] Homitz, J., *A Lean-Premixed Hydrogen Injector with Vane Driven Swirl for Application in Gas Turbines*, in *Mechanical Engineering*, Virginia Tech: Blacksburg, 2006.
- [4] Dahl, G. and Suttrop, F., "Engine Control and Low-NO_x Combustion for Hydrogen Fuelled Aircraft Gas Turbines," *International Journal of Hydrogen Energy*, Vol. 23, No. 8, pp. 695-704, 1998.
- [5] McCarty, R., *Hydrogen: Its Technology and Implications*, Vol. 3 CRC Press: Cleveland, 1975.
- [6] Plee, S. and Mellor, A., "Review of Flashback Reported in Pre vaporizing/Premixing Combustors," *Combustion and Flame*. Vol. 32, pp. 193-203. June 1978.
- [7] Sampath, P. and Shum, F., "Combustion Performance of Hydrogen in a Small Gas Turbine Combustor," *International Journal of Hydrogen Energy*, Vol. 10, No. 12, pp. 829-837, 1985.
- [8] Brand, J. et. al., "Potential Use of Hydrogen in Air Propulsion," *AIAA/ICAS International Air and Space Symposium and Exposition*, Dayton, Ohio, 2003.
- [9] Beerer, D. and McDonnell, V., "Autoignition of Hydrogen and Air Inside a Continuous Flow Reactor with Application to Lean Premixed Combustion," *Journal of Engineering for Gas Turbines and Power*, Vol. 130, No. 5, September 2008.
- [10] Kröner, M., Fritz, J., and Sattelmayer, T., "Flashback Limits for Combustion Induced Vortex Breakdown in a Swirl Burner," *Journal of Engineering for Gas Turbines and Power*, Vol. 125, No. , pp. 693-700, July 2003.
- [11] Minakawa, K., Miyajima, T., and Yuasa, S., "Development of a Hydrogen-Fueled Micro Gas Turbine with a Lean Premixed Combustor," *AIAA/ASME/SAE/ASEE Joint Propulsion Conference & Exhibit*, 33rd, Seattle, WA, 1997.
- [12] LeFebvre, A., *Gas Turbine Combustion*, 2nd ed., Taylor and Francis: Philadelphia, 1999.

- [13] Hill, P. and Peterson, C., *Mechanics and Thermodynamics of Propulsion*, 2nd ed., Addison-Wesley: Reading, 1992.
- [14] NLR (2009), *GSP – Gas Turbine Simulation Program*, Retrieved June 29, 2009, <<http://www.gspteam.com/main/main.shtml>>
- [15] Zucker, R. and Biblarz, O., *Fundamentals of Gas Dynamics*, 2nd ed., John Wiley and Sons: Hoboken, 2002.

Appendix A: Hydrogen-air Premixer Drawings

These drawings are considered proprietary by the sponsor of this research, Electric Jet, LLC. Requests for the drawings should be submitted to:

Electric Jet, LLC.
2000 Kraft Drive Suite 1208
Blacksburg, VA 24060
Phone: 540-552-0824
Email: electricjet@mgwnet.com

Appendix B: Virginia Tech Turbine Laboratory Hydrogen Supply System Setup

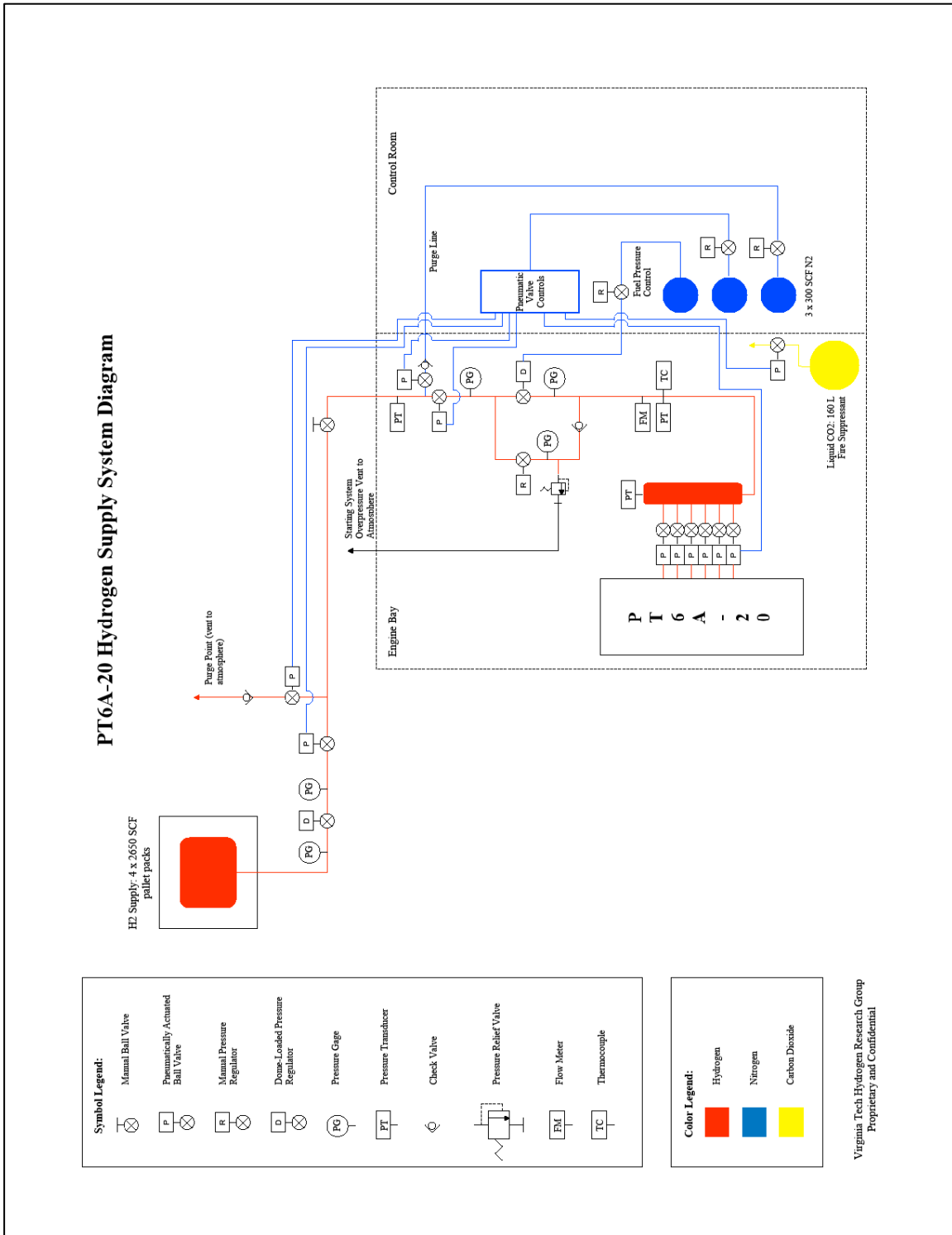


Figure B.1. Detailed schematic of the Virginia Tech Turbine Lab hydrogen supply system

Table B.1. Component list for the airport lab hydrogen supply system

Component	Manufacturer	Model Number
Pneumatically Actuated Ball Valves (Main fuel and purge lines)	Swagelok	SS-65CS16-33O and -33C
Pneumatically Actuated Ball Valves (Fuel manifold to engine)	Swagelok	SS-63TS8-33C
Pressure Gauges	Swagelok	PGI-63B-PG3000-LAQX
Pressure Transducers	Swagelok	PTI-E-NG3000
Check Valves	Swagelok	SS-CHS16-1
Pressure Relief Valve	Swagelok	SS-RL3S4
Solenoid Valves (pneumatic ball valve control)	Swagelok	B- series
Electronic Regulator	Tescom	ER3100
Dome Loaded Regulator	Grove	Mity-Mite Model 90
Hydrogen Meter	Omega	FTB-935

Appendix C: CSDL Test Setup Component List

Table C.1. List of components used in the CSDL test setup

Component	Manufacturer	Model
Primary Air Compressor	Kaeser	FS440
Valve-Control Air Compressor	Ingersoll-Rand	SSR-EP40SE
Air Dryer	Kaeser	KRD-1200
High-Flow Air Valves	Valtek	3000-10
Low-Flow Air Valves	Kammer	25038
Fuel Valves	Valtek	3000-10
Fuel Regulator	Grove	Mity-Mite Series 90
Pilot Regulator	Harris	Model 8700
Air Flow Meters	Eldridge Products	Series 8700-MNPH
Fuel Flow Meters	Eldridge Products	Series 8700-MNPH

Appendix D: Detailed Specifications of the Computer Engine Model

Table D.1. List of component specifications used in the computer engine model

Component	Parameter	Value
Inlet	Air mass flow rate	2.95 kg/s
	Pressure ratio	0.988
	Model standard	MIL-E-5008B
	Map	None
Compressor	Rotor Speed	38,100 rpm
	Pressure Ratio	5.9
	Isentropic Efficiency	0.812
	Model option	Free-state rotor speed
	Map	“compmap”
Combustor	Fuel Flow (Jet-A)	0.0585 kg/s
	Combustion Efficiency	0.95
	Relative Pressure Loss	0.02
Compressor Turbine	Rotor Speed	38,100 rpm
	Isentropic Efficiency	0.85
	Model option	Free-state rotor speed
	Spool inertial moment	0.0683 kg-m ²
	Spool mechanical efficiency	0.990
	Map	“ABFANLPT”
	Power delivered to shaft at design point	All required
Power Turbine	Rotor Speed	33,000 rpm
	Isentropic Efficiency	0.72
	Model option	Power balance at rotor speed
	Spool Inertial Moment	8.08 kg-m ²
	Spool mechanical efficiency	0.990
	Map	“turbmap”
	Power delivered to shaft at design point	All required
Exhaust Nozzle	CD	1.0
	Map	none

Appendix E: Detailed Premixer Operating Conditions at the Flashback Limit

Table E.1. List of operating conditions at which premixer flashback was observed

Upstream Pressure (atm)	Downstream Pressure (atm)	Air Flow (kg/s)	Fuel Flow (kg/s)	Eq. Ratio	Air Temperature (C)	MW at exit (kg/kmol)	Mixture Velocity (m/s)
2.62	2.58	0.0136	0.000317	0.775	133	22.14	63.2
2.79	2.76	0.0149	0.000335	0.750	105	22.29	59.8
3.09	3.06	0.0140	0.000309	0.735	58	22.40	44.5
3.10	3.06	0.0155	0.000372	0.802	130	21.97	60.8
3.11	3.06	0.0154	0.000364	0.786	69	22.05	51.0
3.13	3.06	0.0159	0.000419	0.876	141	21.49	65.2
3.14	3.10	0.0159	0.000415	0.867	62	21.55	52.5
3.32	3.28	0.0167	0.000425	0.851	89	21.65	55.8
3.34	3.30	0.0162	0.000415	0.854	104	21.63	56.3
3.45	3.38	0.0163	0.000459	0.937	132	21.13	60.3
3.45	3.38	0.0174	0.000525	1.002	149	20.75	68.5
3.47	3.39	0.0193	0.000441	0.759	74	22.24	57.8
3.48	3.42	0.0213	0.000388	0.607	145	23.29	72.5
3.59	3.52	0.0192	0.000493	0.854	140	21.63	68.1
3.59	3.54	0.0206	0.000498	0.805	108	21.94	66.2
3.60	3.57	0.0174	0.000506	0.968	98	20.95	57.1
3.63	3.54	0.0197	0.000528	0.891	140	21.40	70.0
3.77	3.68	0.0212	0.000565	0.889	141	21.42	72.3
3.79	3.73	0.0182	0.000516	0.946	65	21.08	51.4
3.81	3.77	0.0176	0.000534	1.007	68	20.73	50.9
3.83	3.74	0.0207	0.000609	0.982	153	20.87	73.5
4.18	4.11	0.0208	0.000602	0.962	69	20.98	54.2
4.38	4.32	0.0205	0.000613	0.998	101	20.78	56.2
4.50	4.37	0.0252	0.000723	0.956	160	21.01	76.9
4.55	4.49	0.0222	0.000631	0.945	75	21.08	53.7
4.78	4.70	0.0219	0.000722	1.096	72	20.24	52.5